Vulnerability of amphibians to global warming

Patrice Pottier[1,2*], Michael R. Kearney[3], Nicholas C. Wu[4], Alex R. Gunderson[5], Julie E. Rej[5], A. Nayelli Rivera-Villanueva[6,7], Pietro Pollo[1], Samantha Burke[1], Szymon M. Drobniak[1,8+], and Shinichi Nakagawa[1,9+]

[1] Evolution & Ecology Research Centre, School of Biological, Earth and Environmental Sciences, University of New South Wales, Sydney, New South Wales, Australia.

[2] Division of Ecology and Evolution, Research School of Biology, The Australian National University, Canberra, Australian Capital Territory, Australia

[3] School of BioSciences, The University of Melbourne, Melbourne, Victoria, Australia

[4] Hawkesbury Institute for the Environment, Western Sydney University, Richmond, New South Wales, Australia

[5] Department of Ecology and Evolutionary Biology, Tulane University, New Orleans, Louisiana, USA

[6] Centro Interdisciplinario de Investigación para el Desarrollo Integral Regional Unidad Durango (CIIDIR), Instituto Politécnico Nacional, Durango, México

[7] Laboratorio de Biología de la Conservación y Desarrollo Sostenible de la Facultad de Ciencias Biológicas, Universidad Autónoma de Nuevo León, Monterrey, México

[8] Institute of Environmental Sciences, Jagiellonian University, Kraków, Poland.

[9] Department of Biological Sciences, University of Alberta, Edmonton, Alberta, Canada.

[*]Corresponding author

[+]These authors supervised the work equally

Corresponding author: Patrice Pottier (p.pottier@unsw.edu.au)

ORCID

Patrice Pottier https://orcid.org/0000-0003-2106-6597

Michael R. Kearney https://orcid.org/0000-0002-3349-8744

Nicholas C. Wu https://orcid.org/0000-0002-7130-1279

Alex R. Gunderson https://orcid.org/0000-0002-0120-4246

Julie E. Rej https://orcid.org/0000-0002-3670-067X

A. Nayelli Rivera-Villanueva https://orcid.org/0000-0002-9190-4317

Pietro Pollo https://orcid.org/0000-0001-6555-5400

Samantha Burke https://orcid.org/0000-0001-6902-974X

Szymon M. Drobniak https://orcid.org/0000-0001-8101-6247

Shinichi Nakagawa https://orcid.org/0000-0002-7765-5182

Main text

Amphibians are the most threatened vertebrates, yet their resilience to rising temperatures remains poorly understood[1,2]. This is primarily because knowledge of thermal tolerance is taxonomically and geographically biased[3], compromising global climate vulnerability assessments. Here, we employed a phylogenetically-informed data imputation approach to predict the heat tolerance of 60% of amphibian species and assessed their vulnerability to daily temperature variation in thermal refugia. We found that 104 out of 5203 species (2%) are currently exposed to overheating events in shaded terrestrial conditions. Despite accounting for heat tolerance plasticity, a 4°C global temperature increase would create a step-change in impact severity, pushing 7.5% of species beyond their physiological limits. In the Southern Hemisphere, tropical species encounter disproportionally more overheating events, while non-tropical species are more susceptible in the Northern Hemisphere. These findings challenge evidence for a general latitudinal gradient in overheating risk[4–6] and underscore the importance of considering climatic variability in vulnerability assessments. We provide conservative estimates assuming access to cool shaded microenvironments. Therefore, the impacts of global warming will likely exceed our projections. Our microclimate-explicit analyses demonstrate that vegetation and water bodies are critical in buffering amphibians during heat waves. Immediate action is needed to preserve and manage these microhabitat features.

Climate change has pervasive impacts on biodiversity, yet the extent and consequences of this environmental crisis vary spatially and taxonomically[7,8]. For ectothermic species, such as amphibians, the link between climate warming and body temperature is clear, with immediate effects on physiological processes[9]. Over 40% of amphibian species are currently listed as threatened, and additional pressures due to escalating thermal extremes may further increase their extinction risk[2,10]. Therefore, it is vital to assess the resilience of amphibians to climate change to prioritise where and how conservation actions are taken.

Accurate assessments of resilience to climate change require adequate data on thermal tolerance and environmental exposure[5,6,11]. However, the most exhaustive dataset on amphibian heat tolerance limits only covers 7.5% of known species and is geographically biased towards temperate regions[3] (Fig. 1). This discrepancy is problematic, considering the high species richness in the tropics and the mounting evidence that tropical ectotherms are most susceptible to rising temperatures[4–6,12,13]. Such sampling biases call into question the reliability of inferences in under-sampled areas and have implications for conservation strategies. Given the rapid pace of climate change and the finite resources available for research, acquiring

sufficient empirical data to fill these knowledge gaps within a realistic timeframe is increasingly untenable[14,15]. Therefore, alternative methods to identify the populations and areas most susceptible to thermal stress are critically needed in a rapidly warming climate.

Climate vulnerability assessments also require environmental data with high spatial and temporal resolution, particularly because extreme heat is more likely to trigger overheating events than increased mean temperatures[16–18]. When heat tolerance limits are known, cutting-edge approaches in biophysical ecology allow fine-scale vulnerability assessments that account for morphology, behaviour, and microhabitat setting in both historical and future climate projections[19,20]. While broadly applicable, biophysically informed analyses are particularly relevant for amphibians, whose body temperatures depend on evaporative heat loss and whose microhabitat use span terrestrial, aquatic, and arboreal environments. Because microenvironmental features are essential for behavioural thermoregulation[21,22], modelling microhabitats allow assessments of the effectiveness of different thermal refugia in buffering the impacts of extreme heat events.

Here, we assess the global vulnerability of amphibians to extreme heat events in different climatic scenarios and thermal refugia (Extended Data Fig. 1). By integrating predicted thermal limits for 60% of amphibian species with daily operative body temperatures, our study offers the first comprehensive evaluation of the impact of heat extremes on the physiological viability of amphibians in nature.

Thermal limits and environmental exposure

We first developed an approach to predict standardised thermal limits for 5,203 amphibian species using data imputation based on phylogenetic niche clustering (Pagel's λ = 0.95 [0.91 – 0.98]) and known correlations between critical thermal limits (CT_{max}) and other variables (n = 2,661 estimates measured in 524 species; Methods). Our phylogenetic model-based imputation approach has expanded our understanding of amphibian thermal tolerance by generating testable predictions for 4,679 unstudied species, particularly in biodiversity hotspots (Fig. 1-2). We confirmed our imputation approach was likely accurate and unbiased by demonstrating a strong congruence between experimental and imputed data in cross-validations (experimental mean ± standard deviation = 36.19 ± 2.67; imputed mean = 35.93 ± 2.54;

n = 375; r = 0.86; Extended Data Fig. 2a,b), though, as expected, the uncertainty in imputed predictions was higher in understudied clades (Extended Data Fig. 2c).

We then integrated predicted thermal limits with daily maximum operative body temperature fluctuations estimated from biophysical models to evaluate the sensitivity of amphibians to extreme heat events in terrestrial, aquatic, and arboreal microhabitats (Extended Data Fig. 1; Methods). Operative body temperatures are the steady-state body temperatures that organisms would achieve in a given microenvironment, which can diverge significantly from ambient air temperatures due to, for example, radiative and evaporative heat exchange processes[19,20]. For each microhabitat, we modelled daily operative body temperatures during the warmest quarters of 2006-2015 and across the distribution range of each species (Methods). We also used projected future climate data from TerraClimate[23] to generate projections assuming 2°C or 4°C of global warming above pre-industrial levels. These temperatures are within the range projected by the end of the century under low and intermediate/high greenhouse gas emission scenarios, respectively[24]. Notably, recent historical CO_2 emissions most closely align with high warming scenarios[25] (i.e., 4.3°C of predicted warming by 2100). All microenvironmental projections assumed access to 85% of shade and sufficient humidity to maintain wet skin to simulate amphibians in thermal refugia (Methods).

We estimated the vulnerability of amphibians by estimating daily differences between predicted thermal limits and maximum hourly operative body temperatures (Extended Data Fig. 1; Methods). We also adjusted daily thermal limits to assume that species were, on any given day, acclimated to local mean weekly operative body temperatures, effectively accounting for plasticity throughout species' distribution ranges (Methods). In total, we predicted vulnerability metrics for 203,853 local species occurrences (individual species in 1° x 1° grid cells) in terrestrial conditions (5,177 species), 204,808 local species occurrences in water bodies (5,203 species); and 56,210 local species occurrences (1,771 species) in above-ground vegetation, for each warming scenario. The number of species examined in arboreal conditions was lower to reflect morphological adaptations required for climbing in above-ground vegetation. These estimates were then grouped into assemblages (all species occurring in 1° x 1° grid cells), tallying 14,090

and 14,091 assemblages for terrestrial and aquatic species and 6,614 assemblages for arboreal species, respectively.

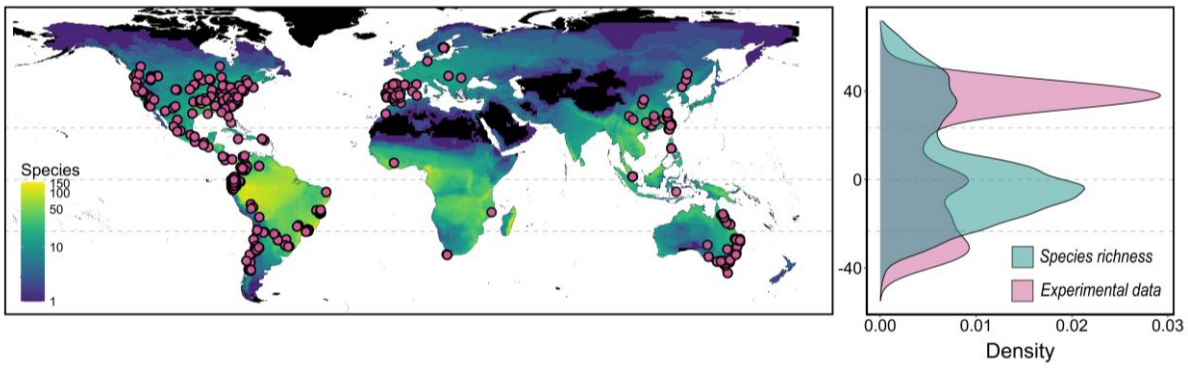

Fig. 1 | Contrast between the geographical locations at which experimental data were collected and patterns in species richness. Pink points denote experimental data (n = 587 species), while the colour gradients refer to species richness calculated in 1 x 1 ° grid cells in the imputed data (n = 5,203 species). Density plots on the right panel represent the distribution of experimental data (pink) and the number of species inhabiting these areas (blue) across latitudes. Dashed lines represent the equator and tropics.

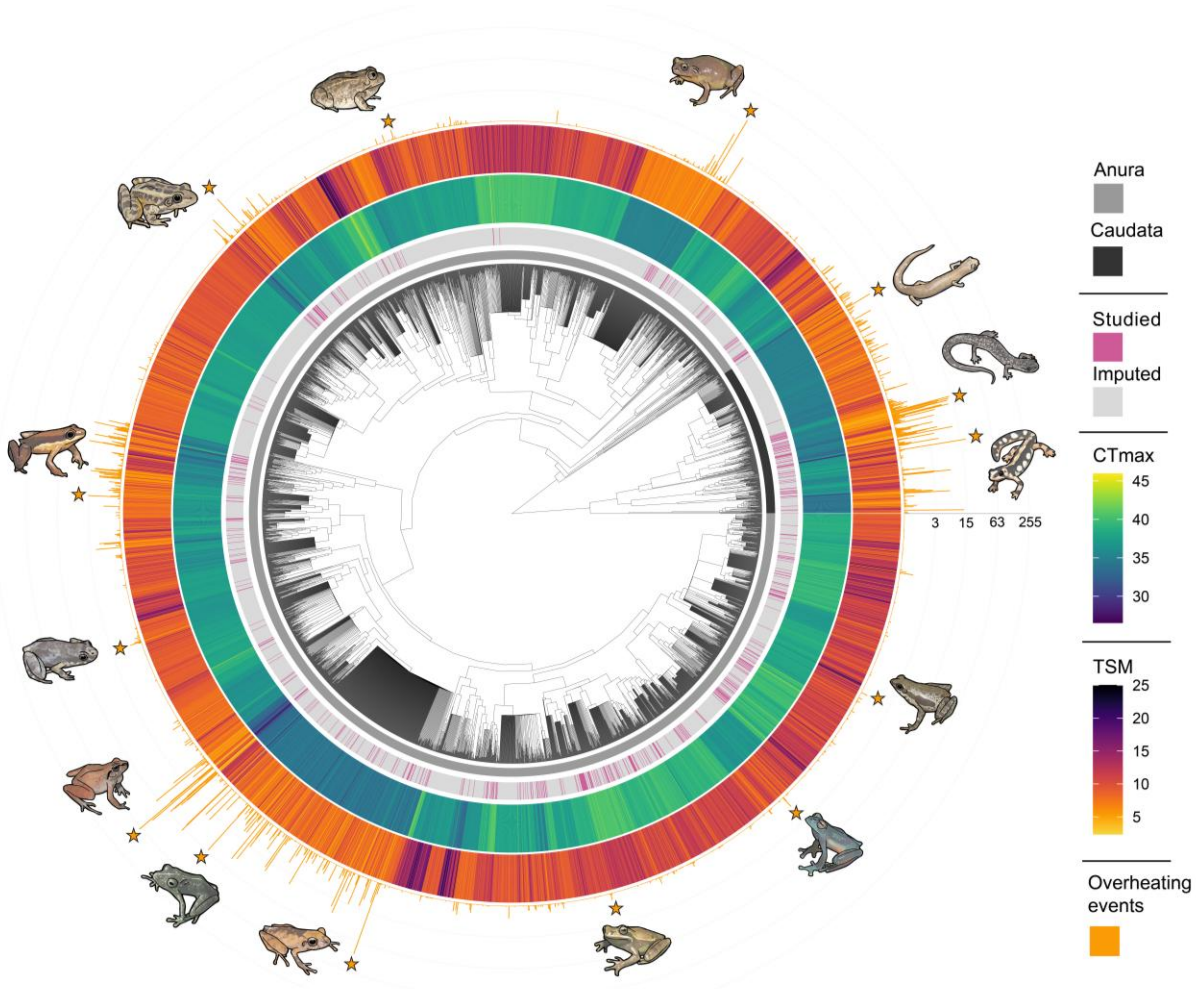

Fig. 2 | Phylogenetic coverage and taxonomic variation in climate vulnerability. Heat maps show heat tolerance limits (CT_{max}) and thermal safety margins (TSM), while histograms show the number of overheating events (days) averaged across each species' distribution range (n = 5,177 species). Pink bars refer to species with prior knowledge (n = 521), while grey bars refer to entirely imputed species (n = 4,656). This figure was constructed assuming ground-level microclimates occurring under 4°C of global warming above pre-industrial levels. Phylogeny is based on the consensus of 10,000 trees sampled from a posterior distribution (see [26] for details). Highlighted species starting from the right side, anti-clockwise: *Neurergus kaiseri* (© Omid Mozaffari), *Plethodon kiamichi* (© Herps of Arkansas), *Bolitoglossa altamazonica* (© Nick Volpe), *Cophixalus aenigma* (© Shane Black), *Tomaptera cryptotis* (© Warwick Tarboton), *Lithobates palustris* (© Herps of Arkansas), *Allobates subfolionidificans* (© Albertina Pimentel Lima), *Phyzelaphryne miriamae* (© Rafael Fraga), *Barycholos ternetzi* (© Werther Ramalho), *Pristimantis carvalhoi* (© William E. Duellman), *Pristimantis ockendeni* (© Albertina Pimentel Lima), *Boana curupi* (© Alfredo Sabaliauskas), *Teratohyla adenocheira* (©André Teles), *Atelopus spumarius* (© Mauricio Vicariotto).

Vulnerability to historical and future heat

We first calculated thermal safety margins (TSM, *sensu* [6]) as the weighted mean difference between heat tolerance limits (CT_{max}) and the maximum daily body temperatures of the warmest quarters of 2006-2015 for each local species occurrence. Thermal safety margins averaged from long-term climatology are routinely used in climate vulnerability analyses[27–29]. We found evidence for a decline in TSM towards mid to low latitudes in all microhabitats, a pattern maintained across warming scenarios (Fig. 3, Extended Data Fig. 3). However, warming substantially reduce TSM at all latitudes (Fig. 3), likely reflecting the contrast between weak plastic responses in CT_{max} across latitudes[11,15] and large variation in environmental temperatures (Extended Data Fig. 3). Across all conditions simulated, TSM is always positive, even in the highest warming scenario (Fig. 3, Extended Data Fig. 3). The mean TSM is lower for terrestrial (mean [95% confidence intervals]; current = 11.69 [8.86 – 14.43]; +4°C = 9.41 [6.53 – 12.09]) and arboreal conditions (current = 12.23 [9.40 – 14.96]; +4°C = 10.07 [7.23 – 12.80]) than for water bodies (current = 13.60 [10.71 – 16.28]; +4°C = 11.68 [8.80 – 14.36]; Fig. 3; Table S1).

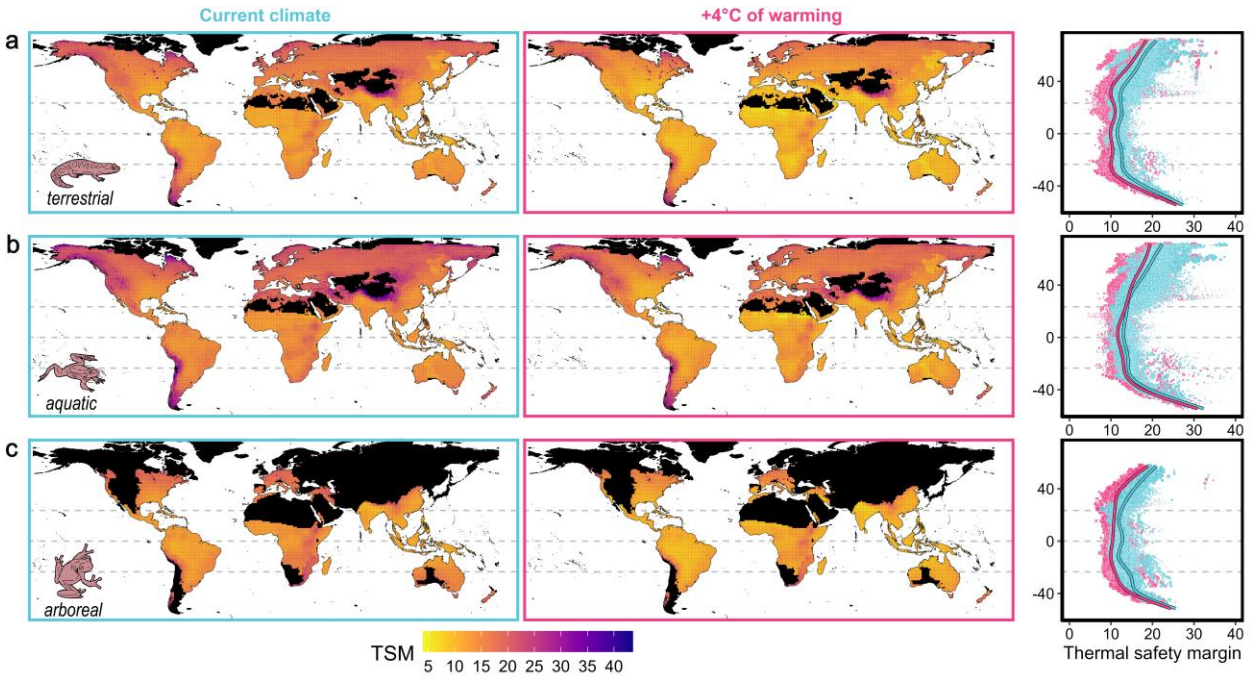

153

154 **Fig. 3 | Assemblage-level patterns in thermal safety margin for amphibians in terrestrial (a), aquatic**
155 **(b) or arboreal (c) microhabitats**. Thermal safety margins (TSM) were calculated as the weighted mean
156 difference between CT_{max} and the predicted operative body temperature in full shade during the warmest
157 quarters of 2006-2015 in each assemblage (1-degree grid cell; n = 14,090 for terrestrial species; n = 14,091
158 for aquatic species; n = 6,614 for arboreal species). Black colour depicts areas with no data. The right panel
159 depicts mean latitudinal patterns in TSM in current climates (blue) or assuming 4°C of global warming
160 above pre-industrial levels (pink), as predicted from generalised additive mixed models. Point estimates are
161 scaled by precision (1/s.e.), with smaller points indicating greater uncertainty. Dashed lines represent the
162 equator and tropics.

163 Because extreme heat events are more likely to trigger overheating events than mean temperatures[5,6,11], we
164 also calculated the binary probability (0/1) that operative body temperatures exceeded CT_{max} for at least
165 one day across the warmest quarters of 2006-2015 (i.e., overheating risk). Overall, overheating risk is low,
166 although numerous species are predicted to face overheating events locally (Fig. 4, Table S2). In terrestrial
167 conditions, we predict that 104 species (836 local species occurrences from 253 assemblages) are likely to
168 experience overheating events in current microclimates (Fig. 4-5). However, under 4°C of warming, 391
169 species (4,248 local species occurrences from 1,328 assemblages) are expected to overheat, which
170 represents nearly a four-fold increase relative to current conditions (Fig. 4-5; Table S2-3). The number of
171 species predicted to overheat in each grid cell also increases with warming; each assemblage comprises up
172 to 18 vulnerable species in current climates (mean [95% confidence intervals] = 3.19 [0.60 – 6.88] species)
173 and up to 37 vulnerable species with 4°C of global warming (3.08 [0.62 – 6.56]; Fig. 4; Table S3). In
174 addition, the proportion of species predicted to experience overheating events in each assemblage varies

175 geographically and between warming scenarios (Extended Data Fig. 5; Table S4). The proportion of species
176 at risk is high in some areas with high species richness (e.g., Northern Australia, Southeastern United States)
177 and not linearly predicted by latitude (Extended Data Fig. 5).

178 In current conditions for species that can shelter in trees (arboreal), 74 assemblages (comprising 1-6 species;
179 1.93 [0.05 – 5.05] species) are predicted to overheat, while 285 assemblages (comprising 1-11 species; 2.51
180 [0.31 – 5.69] species) are predicted to overheat assuming 4°C of global warming (Fig. 4; Table S3). While
181 the overheating risk is lower in arboreal conditions, considerably fewer species were examined than in
182 terrestrial conditions (1,771 vs. 5,177 species). In fact, comparing the responses of arboreal species in
183 different microhabitats revealed that occupying above-ground vegetation is only partially beneficial
184 (Extended Data Fig. 4). In current climates, up to 15 arboreal species (320 local species occurrences) are
185 predicted to experience overheating events in terrestrial conditions, whereas 13 arboreal species (152 local
186 species occurrences) are predicted to overheat in above-ground vegetation (Extended Data Fig. 4).
187 Furthermore, under 4°C of warming, 83 arboreal species (1,137 local species occurrences) are predicted to
188 overheat in terrestrial conditions, while retreating to above-ground vegetation only reduces the number of
189 species exposed to overheating events by 32.5% (56 species, 748 local species occurrences) (Extended Data
190 Fig. 4). Contrary to terrestrial and arboreal conditions, no amphibian populations are predicted to overheat
191 in water bodies in current or intermediate climate warming scenarios due to the thermal buffering properties
192 of water. However, assuming 4°C of climate warming, we predict that 11 species (56 local species
193 occurrences from 48 assemblages) will exceed their physiological limits in aquatic microhabitats (Fig. 4).

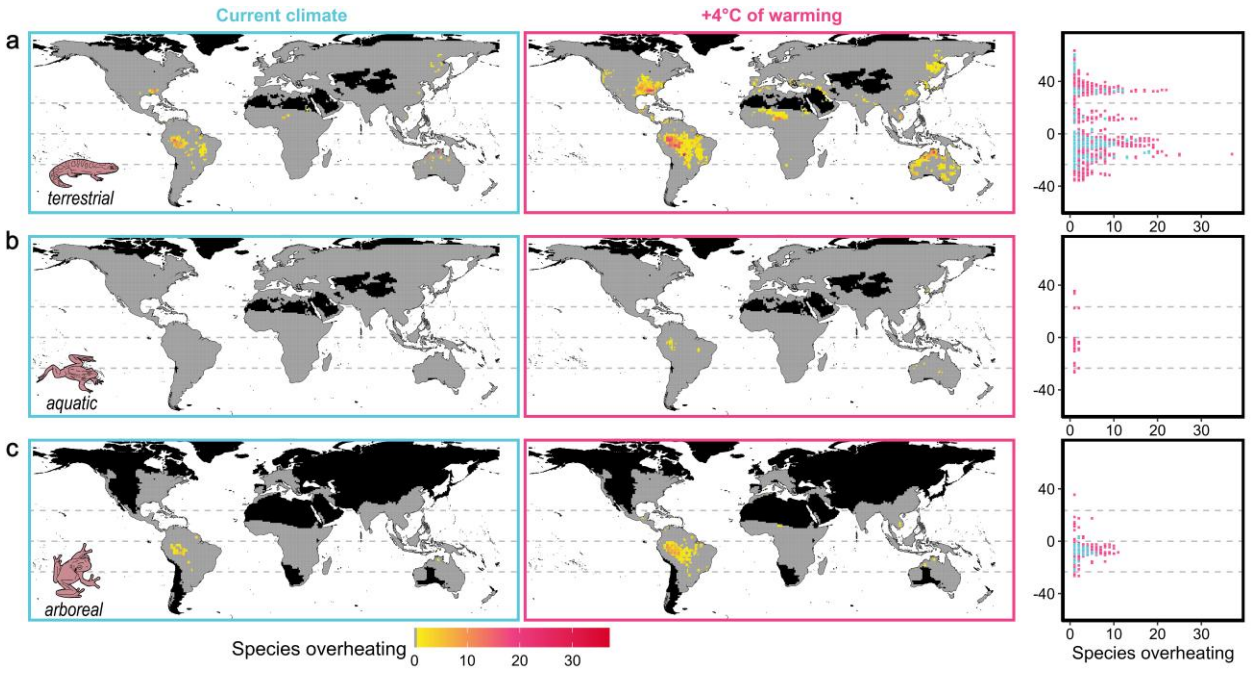

Fig. 4 | Number of species predicted to experience overheating events in terrestrial (a), aquatic (b), and arboreal (c) microhabitats. The number of species overheating was assessed as the sum of species overheating for at least one day in the period surveyed (warmest quarters of 2006-2015) in each assemblage (1-degree grid cell; n = 14,090 for terrestrial species; n = 14,091 for aquatic species; n = 6,614 for arboreal species). Black colour depicts areas with no data, and grey colour assemblage without species at risk of overheating. The right panel depicts latitudinal patterns in the number of species predicted to overheat in current climates (blue) or assuming 4°C of global warming above pre-industrial levels (pink). Dashed lines represent the equator and tropics.

Finally, we quantified the number of days (out of 910 simulated days across the warmest quarters of 2006-2015) each species was predicted to locally exceed their plasticity-adjusted heat tolerance limits. This metric fully integrates the frequency at which amphibians are predicted to experience temperatures beyond their thermal limits. For current climates, we found that species rarely experience overheating events in shaded terrestrial conditions (overall mean overheating days [95% confidence intervals] = 0.01 [0.01 – 0.08]; mean among overheating species = 2.15 [0.24 – 5.26] days); but these figures increase considerably with global warming (Fig. 5; Table S2). Under 4°C of warming, species are predicted to overheat on as many as 207.18 [182.39 – 231.97] days, representing up to 22.8% of the warmest days of the year (overall mean = 0.15 [0.05 – 0.46] days; mean among overheating species = 6.75 [3.14 – 11.38] days; Fig. 5; Table S2). This is noticeably more than what is predicted under 2°C of warming (overall mean = 0.02 [0.01 – 0.13] days; mean among overheating species = 2.58 [0.41 – 5.86] days; Fig. 5; Table S2). In above-ground vegetation, the frequency of overheating events is lower, as expected. Under current climates, arboreal

species are predicted to overheat on up to 5.65 [1.00 – 10.29] days in total (overall mean = 0.01 [0.01 – 0.04] days; mean among overheating species = 1.62 [0.03 – 4.43] days; Fig. 5; Tab. Table S2). Under 4 degrees of warming, arboreal species are predicted to overheat on up to 76.17 [59.79 – 92.54] days (overall mean = 0.08 [0.01 – 0.23] days; mean among overheating species = 5.08 [1.81 – 9.39] days; Fig. 5; Table S2). Arboreal species retreating to above-ground vegetation are predicted to experience fewer overheating events than those in terrestrial conditions (Extended Data Fig. 4). Interestingly, we found that species predicted to overheat locally have TSMs well above zero, although some are living particularly close to their heat tolerance limits during the warmest months in both terrestrial (mean [95% confidence intervals]; current = 8.20 [6.91 – 9.98], range: 3.02 – 12.19; +4°C = 6.30 [5.02 – 8.09], range: 0.97 – 11.27) and above-ground conditions (current = 8.71 [7.20 – 10.28], range: 3.70 – 9.76; +4°C = 6.73 [5.44 – 8.48], range: 1.75 – 8.70; Fig. 5c,d). Finally, we found a strong non-linear negative association between the number of overheating events and the thermal safety margin, with stark contrasts between warming scenarios (Fig. 5c,d; Table S5). In particular, overheating days increase rapidly as thermal safety margins fall below 5°C (Figure 5c,d).

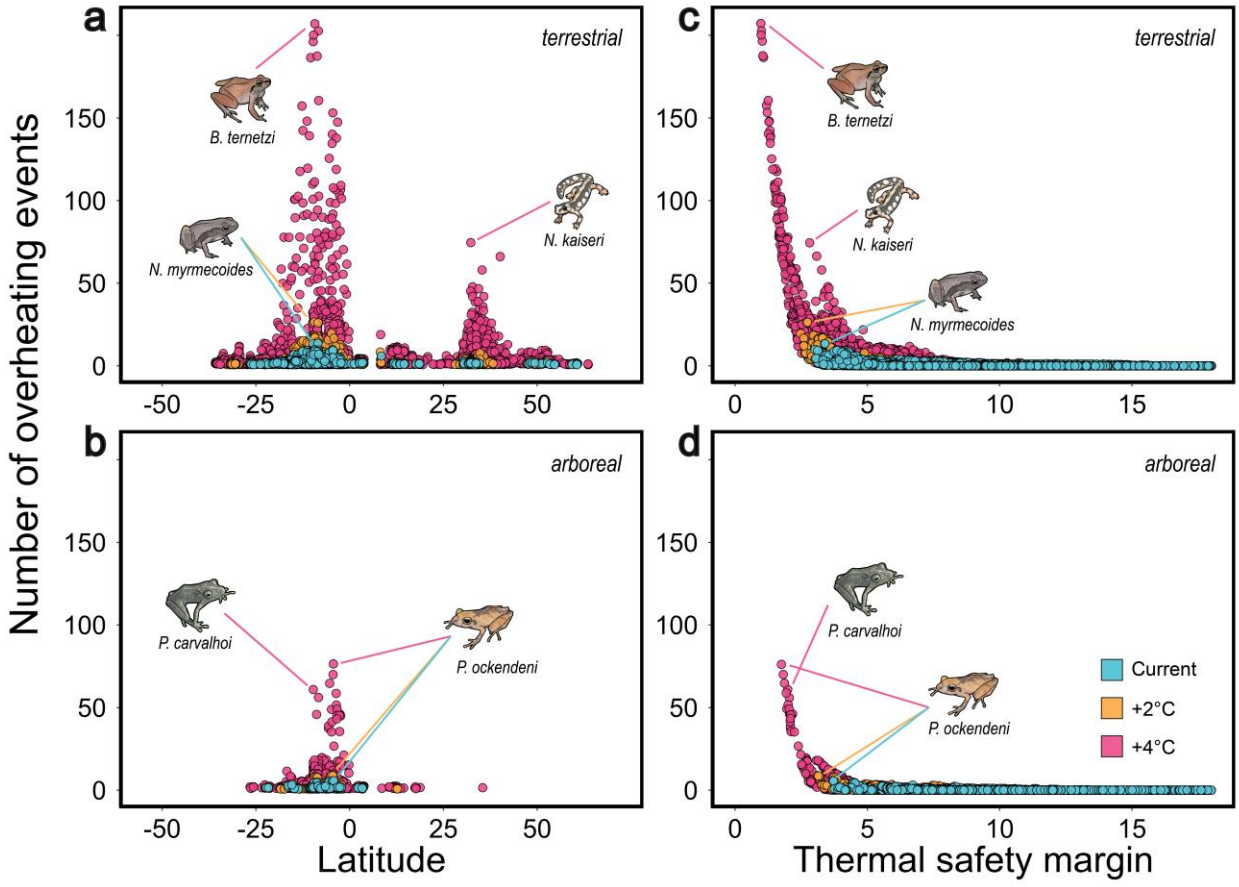

Fig. 5 | Latitudinal variation in the number of overheating events in terrestrial (a,c) and arboreal (b,d) microhabitats as a function of latitude (a,b) and thermal safety margin (c,d). The number of overheating events (days) were calculated based on the mean probability that daily maximum temperatures exceeded CT_{max} during the warmest quarters of 2006-2015 for each species in each grid cell (i.e., local species occurrences; n = 203,853 for terrestrial species; n = 204,808 for aquatic species; n = 56,210 for aquatic species). Blue points depict the number of overheating events in current microclimates, while orange and pink points depict the number of overheating events assuming 2°C and 4°C of global warming above pre-industrial levels, respectively. For clarity, only the species predicted to experience at least one overheating event are depicted across latitudes (a,b). Highlighted species are: *Neurergus kaiseri* (© Omid Mozaffari), *Noblella myrmecoides* (© Dante Fenolio), *Barycholos ternetzi* (© Werther Ramalho), *Pristimantis carvalhoi* (© William E. Duellman), *Pristimantis ockendeni* (©Albertina Pimentel Lima).

The mounting impacts of global warming

Quantifying the resilience of biodiversity to a changing climate is one of the most pressing challenges for contemporary science[7,8]. Here, we show that over a hundred species may already experience hourly temperatures that would likely result in death over minutes or hours of exposure in thermal refugia. This pattern is only predicted to worsen (Fig. 4-5). Assuming 4°C of global warming, the number of species and assemblages exposed to overheating events would be four to five times higher than currently, totalling 391 out of 5,203 species studied (7.5%; Fig. 4-5).

We also found striking disparities in overheating risk between the 2°C and 4°C warming projections (Fig. 5; Table S1), which are anticipated by the end of the century under low and high greenhouse gas emission scenarios, respectively[24]. The more extreme warming scenario considerably increased the number overheating events experienced by amphibian populations (Fig. 5), highlighting the escalating and abrupt impacts of global warming[7,30]. Such an increase is attributable to the contrast between the rapid pace at which temperatures are increasing and the low ability of amphibians to acclimate to new thermal environments via plasticity (Extended Data Fig. 3; species-level acclimation response ratio ± s.d. = 0.134 ± 0.008). Our study clearly demonstrates, as others have suggested[18,28,31,32], that physiological plasticity is not a sufficient mechanism to buffer many populations from the impacts of rapidly rising temperatures.

Extreme heat events drive vulnerability

We found large spatial heterogeneity in the vulnerability of amphibians. In tropical areas, most vulnerable species are concentrated in South America and Australia, whereas fewer species are impacted in the African

and Asian tropics (Fig. 4). Tropical species also experience disproportionately more overheating events in the Southern Hemisphere, while non-tropical species are more susceptible in the Northern Hemisphere (Fig. 5). Furthermore, the proportion of species experiencing overheating events in each assemblage was not predicted by latitude (Extended Data Fig. 5). Therefore, our findings are inconsistent with the expectation of a general latitudinal gradient in overheating risk based on thermal safety margins[4–6,13]. In fact, the overheating risk does not increase linearly with TSM (Fig. 5c,d), and species with seemingly comparable TSMs can have markedly different probabilities of overheating due to varying exposure to daily temperature fluctuations (Fig. 5c,d). Therefore, TSMs alone hide critical tipping points for thermal stress (Fig. 5c,d).

Our study questions the reliability of thermal safety margins and other climate vulnerability metrics when averaged across large time scales (e.g., using the maximum temperature of the warmest quarter) for detecting species most vulnerable to thermal extremes. It also challenges the general notion that low-latitude species are uniformly most vulnerable to warming[4–6,13], revealing a far more nuanced pattern of climate vulnerability across latitudes. While the reliability of TSM-based assessments has been questioned in previous studies[11], our work further emphasises the need to consider natural climatic variability and extreme hourly temperatures[4,16–18] when evaluating the vulnerability of ectotherms to global warming. Considering alternative metrics, such as the number of predicted overheating events, may prove particularly useful in identifying the most vulnerable species and populations.

The vital yet limited role of thermal retreats

Our study highlights the critical yet sometimes insufficient role that thermal retreats play in buffering the impacts of warming on amphibians. Most amphibian species are predicted not to experience overheating events in full shade (Fig. 4), and the availability of water bodies allows nearly all amphibians to maintain their body temperatures below critical levels, apart from 11 species in the most extreme warming scenario investigated. This is attributable to the higher specific heat capacity of water relative to air, delaying rapid temperature rises and affording a more stable environment during heat waves[33]. Our findings add to the growing evidence that finding access to cooler microhabitats is the main strategy amphibians and other ectotherms can use to maintain sub-lethal body temperatures[6,21,34].

However, it is crucial to emphasise that vegetated terrestrial conditions in full shade offer inadequate protection to 7.5% of species, and many arboreal species predicted to overheat at ground level face similar risks in above-ground vegetation (Fig. 4-5, Extended Data Fig. 4). In fact, although reducing the frequency of overheating events (Extended Data Fig. 4), access to shaded above-ground vegetation only reduces the number of vulnerable species by 32.5%. Moreover, although burrows offer cooler microclimates (see Extended Data Fig. 9), the ability to use underground spaces is not universal among amphibians and can greatly restrict activity, reproduction, and foraging opportunities.

Warming impacts may exceed projections

Our predictions are largely conservative, and likely overestimate the resilience of amphibians to global warming in two main ways. First, we assume that microhabitats such as shaded ground-level substrates, above-ground vegetation, and water bodies are available throughout a species' range, and that amphibians can maintain wet skin. These assumptions will often be violated as habitats are degraded. Deforestation and urbanization are diminishing vital shaded areas[35,36], while increased frequencies of droughts will cause water bodies to evaporate[37,38]. These changes compromise not only habitat integrity but also local humidity levels – key for effective thermoregulation[39,40]. Consequently, amphibians will likely experience higher body temperatures and desiccation stress events than our models predict due to inconsistent access to cooler microhabitats[41], particularly in degraded systems.

Second, ectotherms can experience deleterious effects from heat stress before reaching their heat tolerance limits. Prolonged exposure to sub-lethal temperatures can lead to altered activity windows[42,43], disruptions to phenology[44,45], reduced reproductive fitness (fertility and fecundity)[29,46,47], and death[48,49]. Although comprehensive data on thermal incapacitation times and fertility impacts are sparse in amphibians, integrating both the duration and intensity of thermal stress[49–51] will likely point to more extreme vulnerability estimates. This represents a vital avenue for future research, albeit one requiring a large collection of empirical data.

Alternatively, species that can retreat underground during heat events are likely to experience fewer overheating events than our models predict (see Extended Data Fig. 9), and prolonged exposure to high temperatures in the permissive range (*sensu* [48]) can enhance performance and fitness, thereby reducing the

impacts of extreme heat on natural populations. In addition, some species may adapt to changing temperatures. However, evidence for slow rates of evolution and physiological constraints on thermal tolerance[52,53] challenges the likelihood of local adaptation to occur in rapidly warming climates.

The power of data imputation

Our imputation approach has generated testable predictions of the thermal limits of 5,203 species, expanding the scope of previous research[3] (Fig. 2). We also addressed geographical biases by generating predictions in under-sampled but ecologically critical regions of Africa, Asia, and South America (Fig. 2). We found that these understudied regions frequently harbor species exhibiting the highest susceptibility to extreme heat events (Fig. 1,4-5), with 74% (288 out of 391) of vulnerable species remaining unstudied. Targeted research efforts in these vulnerability hotspots are instrumental in validating our model predictions and advancing our understanding of amphibian thermal physiology to inform their conservation. Though undeniable logistical and financial challenges exist in accessing some of these remote locations, collaboration with local scientists could expedite data collection and result in timely conservation measures. Exemplary initiatives to sample numerous species in South America (e.g., [22,54,55]) are promising steps in this direction, and we hope our findings will catalyse research activity in these regions.

Amphibian biodiversity in a warming world

Our study highlights the dire consequences of global warming on amphibians. Yet it is crucial to differentiate between global extinction and local extirpations – the latter being confined extinctions within specific geographic areas. Most species will not experience overheating events throughout their entire range, and these overheating events may not occur simultaneously. Hence, most species are likely to only experience local extirpation due to overheating, according to our models. Nevertheless, local extirpations carry their own sets of ecological repercussions, such as reshuffling community compositions and eroding genetic and ecological diversity[56,57].

Some amphibian populations may also undergo range shifts, permanently or transiently relocating to habitats with more hospitable weather patterns[58]. However, this is only possible if suitable habitats are available for establishment. Given the low dispersal rates of some amphibians and their common reliance

on water bodies for reproduction and thermoregulation, opportunities for range shifts are likely to be rare for many species. Identifying which species at high risk of overheating are simultaneously predicted to have limited ability to extend their range is an interesting avenue for research. In addition, we stress that amphibians living close to their physiological limits for extended times at the warm edge of their distribution are likely to experience heat stress that could hamper activity, foraging opportunities, and reproductive success, adding layers of complexity to their survival challenges and potentially leading to population declines[42,48].

Overall, our study contributes to the evidence that climate change is a mounting threat to amphibians[2,10] and emphasises the importance of limiting global temperature rises below 2°C to minimise the risk of overheating to amphibian populations. A 4°C temperature rise would not just increase these risks but create a step-change in impact severity (e.g., Fig. 5c). The mechanistic basis of our species- and habitat-specific predictions also leads to clear management priorities. Particularly, our analyses revealed the critical importance of preserving dense vegetation cover and water bodies. These microhabitats provide conditions with cooler and more stable temperatures and increase the potential for amphibians and other ectothermic species to disperse to more suitable microhabitats. Establishing protected areas and undertaking habitat restoration initiatives may support amphibians in a changing climate and buffer additional anthropogenic threats, in turn mitigating amphibian population declines[2,10,59]. These actions are critical for the amphibians at risk and the ecosystems they support[60] in a planet undergoing perilous climatic changes.

Main references

1. Carey, C. & Alexander, M. A. Climate change and amphibian declines: is there a link? *Divers. Distrib.* **9**, 111–121 (2003).
2. Luedtke, J. A. *et al.* Ongoing declines for the world's amphibians in the face of emerging threats. *Nature* **622**, 308–314 (2023).
3. Pottier, P. *et al.* A comprehensive database of amphibian heat tolerance. *Sci. Data* **9**, 600 (2022).
4. Pinsky, M. L., Eikeset, A. M., McCauley, D. J., Payne, J. L. & Sunday, J. M. Greater vulnerability to warming of marine versus terrestrial ectotherms. *Nature* **569**, 108–111 (2019).
5. Deutsch, C. A. *et al.* Impacts of climate warming on terrestrial ectotherms across latitude. *Proc. Natl. Acad. Sci. U.S.A.* **105**, 6668–6672 (2008).
6. Sunday, J. M. *et al.* Thermal-safety margins and the necessity of thermoregulatory behavior across latitude and elevation. *Proc. Natl. Acad. Sci. U.S.A.* **111**, 5610–5615 (2014).
7. Urban, M. C. Accelerating extinction risk from climate change. *Science* **348**, 571–573 (2015).
8. Walther, G.-R. *et al.* Ecological responses to recent climate change. *Nature* **416**, 389–395 (2002).
9. Angilletta, M. J. Thermal adaptation: a theoretical and empirical synthesis. (Oxford University Press, 2009).
10. Mi, C. *et al.* Global Protected Areas as refuges for amphibians and reptiles under climate change. *Nat. Commun.* **14**, 1389 (2023).
11. Clusella-Trullas, S., Garcia, R. A., Terblanche, J. S. & Hoffmann, A. A. How useful are thermal vulnerability indices? *Trends Ecol. Evol.* **36**, 1000–1010 (2021).
12. Huey, R. B. *et al.* Why tropical forest lizards are vulnerable to climate warming. *Proc. R. Soc. B* **276**, 1939–1948 (2009).
13. Comte, L. & Olden, J. D. Climatic vulnerability of the world's freshwater and marine fishes. *Nat. Clim. Change* **7**, 718–722 (2017).
14. Carvalho, R. L. *et al.* Pervasive gaps in Amazonian ecological research. *Curr. Biol.* **33**, 3495-3504.e4 (2023).
15. Nesi, P., Luiselli, L. M. & Vignoli, L. "Heaven" of Data Deficient Species: The Conservation Status of the Endemic Amphibian Fauna of Vietnam. *Diversity* **15**, 872 (2023).
16. Müller, J. *et al.* Weather explains the decline and rise of insect biomass over 34 years. *Nature* **628**, 349–354 (2024).
17. Murali, G., Iwamura, T., Meiri, S. & Roll, U. Future temperature extremes threaten land vertebrates. *Nature* **615**, 461–467 (2023).
18. Gunderson, A. R., Dillon, M. E. & Stillman, J. H. Estimating the benefits of plasticity in ectotherm heat tolerance under natural thermal variability. *Funct. Ecol.* **31**, 1529–1539 (2017).
19. Anderson, R. O., White, C. R., Chapple, D. G. & Kearney, M. R. A hierarchical approach to understanding physiological associations with climate. *Glob. Ecol. Biogeogr.* **31**, 332–346 (2022).

20. Briscoe, N. J. *et al.* Mechanistic forecasts of species responses to climate change: The promise of biophysical ecology. *Glob. Change Biol.* **29**, 1451–1470 (2023).
21. Kearney, M., Shine, R. & Porter, W. P. The potential for behavioral thermoregulation to buffer "cold-blooded" animals against climate warming. *Proc. Natl. Acad. Sci. U.S.A.* **106**, 3835–3840 (2009).
22. Duarte, H. *et al.* Can amphibians take the heat? Vulnerability to climate warming in subtropical and temperate larval amphibian communities. *Glob. Change Biol.* **18**, 412–421 (2012).
23. Abatzoglou, J. T., Dobrowski, S. Z., Parks, S. A. & Hegewisch, K. C. TerraClimate, a high-resolution global dataset of monthly climate and climatic water balance from 1958–2015. *Sci. Data* **5**, 170191 (2018).
24. Masson-Delmotte, V. *et al.* Climate change 2021: the physical science basis. *Contribution of working group I to the sixth assessment report of the intergovernmental panel on climate change* **2**, (2021).
25. Schwalm, C. R., Glendon, S. & Duffy, P. B. RCP8.5 tracks cumulative CO2 emissions. *Proc. Natl. Acad. Sci. U.S.A.* **117**, 19656–19657 (2020).
26. Jetz, W. & Pyron, R. A. The interplay of past diversification and evolutionary isolation with present imperilment across the amphibian tree of life. *Nat Ecol Evol* **2**, 850–858 (2018).
27. Clusella-Trullas, S., Blackburn, T. M. & Chown, S. L. Climatic Predictors of Temperature Performance Curve Parameters in Ectotherms Imply Complex Responses to Climate Change. *Am. Nat.* **177**, 738–751 (2011).
28. Morley, S. A., Peck, L. S., Sunday, J. M., Heiser, S. & Bates, A. E. Physiological acclimation and persistence of ectothermic species under extreme heat events. *Glob. Ecol. Biogeogr.* **28**, 1018–1037 (2019).
29. van Heerwaarden, B. & Sgrò, C. M. Male fertility thermal limits predict vulnerability to climate warming. *Nat. Commun.* **12**, 2214 (2021).
30. Trisos, C. H., Merow, C. & Pigot, A. L. The projected timing of abrupt ecological disruption from climate change. *Nature* **580**, 496–501 (2020).
31. Gunderson, A. R. & Stillman, J. H. Plasticity in thermal tolerance has limited potential to buffer ectotherms from global warming. *Proc. R. Soc. B* **282**, 20150401 (2015).
32. Pottier, P. *et al.* Developmental plasticity in thermal tolerance: Ontogenetic variation, persistence, and future directions. *Ecol. Lett.* **25**, 2245–2268 (2022).
33. Denny, M. W. Thermal Properties: Body temperatures in Air and Water. in *Air and Water: The biology and physics of life's media* 145–173 (Princeton University Press, Princeton, New Jersey, USA, 1993).
34. Scheffers, B. R., Edwards, D. P., Diesmos, A., Williams, S. E. & Evans, T. A. Microhabitats reduce animal's exposure to climate extremes. *Glob. Change Biol.* **20**, 495–503 (2014).

35. Stark, G., Ma, L., Zeng, Z.-G., Du, W.-G. & Levy, O. Cool shade and not-so-cool shade: How habitat loss may accelerate thermal stress under current and future climate. *Glob. Change Biol.* **29**, 6201–6216 (2023).
36. Nowakowski, A. J. *et al.* Tropical amphibians in shifting thermal landscapes under land-use and climate change. *Conserv. Biol.* **31**, 96–105 (2017).
37. Dai, A. Increasing drought under global warming in observations and models. *Nat. Clim. Change* **3**, 52–58 (2013).
38. McMenamin, S. K., Hadly, E. A. & Wright, C. K. Climatic change and wetland desiccation cause amphibian decline in Yellowstone National Park. *Proc. Natl. Acad. Sci. U.S.A.* **105**, 16988–16993 (2008).
39. Greenberg, D. A. & Palen, W. J. Hydrothermal physiology and climate vulnerability in amphibians. *Proc. R. Soc. B* **288**, 20202273 (2021).
40. Cheng, C.-T. *et al.* Open habitats increase vulnerability of amphibian tadpoles to climate warming across latitude. *Glob. Ecol. Biogeogr.* **32**, 83–94 (2023).
41. Wu, N. C. *et al.* Global exposure risk of frogs to increasing environmental dryness. Preprint at https://doi.org/10.32942/X2ZG7S (2024).
42. Kearney, M. R. Activity restriction and the mechanistic basis for extinctions under climate warming. *Ecol. Lett.* **16**, 1470–1479 (2013).
43. Enriquez-Urzelai, U. *et al.* The roles of acclimation and behaviour in buffering climate change impacts along elevational gradients. *J. Anim. Ecol.* **89**, 1722–1734 (2020).
44. Enriquez-Urzelai, U., Nicieza, A. G., Montori, A., Llorente, G. A. & Urrutia, M. B. Physiology and acclimation potential are tuned with phenology in larvae of a prolonged breeder amphibian. *Oikos* **2022**, e08566 (2022).
45. Parmesan, C. Ecological and Evolutionary Responses to Recent Climate Change. *Annu. Rev. Ecol. Evol. Syst.* **37**, 637–669 (2006).
46. Wang, W. W.-Y. & Gunderson, A. R. The Physiological and Evolutionary Ecology of Sperm Thermal Performance. *Front. Physiol.* **13**, (2022).
47. Walsh, B. S. *et al.* The Impact of Climate Change on Fertility. *Trends Ecol. Evol.* **34**, 249–259 (2019).
48. Jørgensen, L. B., Ørsted, M., Malte, H., Wang, T. & Overgaard, J. Extreme escalation of heat failure rates in ectotherms with global warming. *Nature* **611**, 93–98 (2022).
49. Rezende, E. L., Castañeda, L. E. & Santos, M. Tolerance landscapes in thermal ecology. *Funct. Ecol.* **28**, 799–809 (2014).
50. Garcia, R. A., Allen, J. L. & Clusella-Trullas, S. Rethinking the scale and formulation of indices assessing organism vulnerability to warmer habitats. *Ecography* **42**, 1024–1036 (2019).

51. Jørgensen, L. B., Malte, H., Ørsted, M., Klahn, N. A. & Overgaard, J. A unifying model to estimate thermal tolerance limits in ectotherms across static, dynamic and fluctuating exposures to thermal stress. *Sci. Rep.* **11**, 12840 (2021).
52. Bennett, J. M. *et al.* The evolution of critical thermal limits of life on Earth. *Nat. Commun.* **12**, 1198 (2021).
53. Morgan, R., Finnøen, M. H., Jensen, H., Pélabon, C. & Jutfelt, F. Low potential for evolutionary rescue from climate change in a tropical fish. *Proc. Natl. Acad. Sci. U.S.A.* **117**, 33365–33372 (2020).
54. May, R. von *et al.* Thermal physiological traits in tropical lowland amphibians: Vulnerability to climate warming and cooling. *PLOS One* **14**, e0219759 (2019).
55. Bovo, R. P. *et al.* Beyond Janzen's Hypothesis: How Amphibians That Climb Tropical Mountains Respond to Climate Variation. *Integr. Org. Biol.* **5**, obad009 (2023).
56. Arenas, M., Ray, N., Currat, M. & Excoffier, L. Consequences of Range Contractions and Range Shifts on Molecular Diversity. *Mol. Biol. Evol.* **29**, 207–218 (2012).
57. Rogan, J. E. *et al.* Genetic and demographic consequences of range contraction patterns during biological annihilation. *Sci. Rep.* **13**, 1691 (2023).
58. Blaustein, A. R. *et al.* Direct and Indirect Effects of Climate Change on Amphibian Populations. *Diversity* **2**, 281–313 (2010).
59. Nowakowski, J. A. *et al.* Protected areas slow declines unevenly across the tetrapod tree of life. *Nature* **622**, 101–106 (2023).
60. Hocking, D. & Babbitt, K. Amphibian Contributions to Ecosystem Services. *Herpetol. Conserv. Biol.* (2014).

Methods

Reporting

We report author contributions using the CRediT (Contributor Roles Taxonomy) statement[61] and MeRIT (Method Reporting with Initials for Transparency) guidelines[62]. We also crafted the study title, abstract and keywords to maximise indexing in search engines and databases[63]. All analyses were performed using R statistical software[64] (v. 4.3.0), and most computations used the computational cluster Katana supported by Research Technology Services at UNSW Sydney. Maps, phylogenetic trees, and data visualisations were generated using the R packages rnaturalearthhires[65], ggtree[66], and ggplot2[67].

Amphibian heat tolerance limits

We leveraged the most comprehensive compilation of amphibian heat tolerance limits[3] for our analyses (Extended Data Fig. 1). Briefly, these data were collated by systematically reviewing the literature in five databases and seven languages, comprising 3,095 heat tolerance limits from 616 amphibian species. To facilitate the comparability and analysis of heat tolerance limits, we only included data matching four specific criteria. First, we only included heat tolerance limits measured using a dynamic methodology (i.e., temperature at which animals lose their motor coordination when exposed to ramping temperatures, critical thermal maximum CT_{max}[68]) because it was the most used and comparable metric. Second, we only selected data for which the laboratory acclimation temperature, or the field temperature during the month of capture, was recorded. Third, we only included data from species listed in the phylogeny from [26]. Fourth, we only included species for which their geographical range was reported in the International Union for the Conservation of Nature red list[69] (accessed in January 2023).

These criteria were chosen to perform phylogenetically, climatically, and spatially informed analyses. In total, we selected 2,661 heat tolerance limits estimates with metadata for 524 amphibian species (mean = 5.08; range = 1 - 146 estimates per species; 287 species with more than one estimate). We also complemented this dataset with ecotypic data for each species. Amphibians were grouped into six major ecotypes according to [41]: ground-dwelling, fossorial, aquatic, semi-aquatic, stream-dwelling and arboreal. Cave specialists were excluded because they experience unique microclimatic conditions.

Data-deficient species

Our objective was to assess the thermal tolerance of amphibians globally. However, the data compiled in [3] are geographically and taxonomically biased. Therefore, we employed a data imputation procedure to infer the thermal tolerance of data-deficient species, totalling 5,203 species at a broad geographical coverage (524 species + 4,679 data-deficient species; ~60% of all described amphibian species, amphibiaweb.org; accessed in December 2023). We selected data-deficient species from a species list that matched the phylogeny from [26] (7,238 species), was listed in the IUCN red list[69] along with geographic distribution data (5,792 species), and for which ecotypes were known (6,245 species). We did not consider Caecilians (order Gymnophiona) because, to our knowledge, heat tolerance limits are unknown for all Caecilian species[3]. Of the 5,792 species for which we had distribution and phylogenetic data, 5,268 were data-deficient for CT_{max}, of which 4,822 had a known ecotype. After removing Caecilians, we were left with 4,679 species to impute. We also supplemented our dataset with published body mass data retrieved from literature sources or estimated based on length-mass allometries[41,70,71]. We then estimated the geographical coordinates at which all extant species occurred in their IUCN distribution range at a 1° x 1° resolution to use for biophysical modelling (Extended Data Fig. 1).

Data imputation

We developed a phylogenetic imputation procedure, here named Bayesian Augmentation with Chained Equations (BACE). The BACE procedure combines the powers of Bayesian data augmentation and multiple imputation with chain equations (MICE[72]). Briefly, we ran multiple iterative models using *MCMCglmm*[73] (v. 2.34) and supporting functions from the *hmi* package[74]. In the first cycle, missing data was either taken as the arithmetic mean for continuous predictors, or randomly sampled from existing values for (semi)categorical predictors. Predicted (augmented) values from the models were then extracted from the response variables and used as predictor variables in the next models to predict other response variables. Ultimately, heat tolerance limits were predicted using augmented data from all predictors. We ran 5 cycles where the data from one cycle was iteratively used in the next cycle, and estimations converged after the first cycle. Although the proportion of missing data was large (89.9%), imputations based on large amounts of missing data are common[13,75], and although estimate uncertainty increases with the proportion

of missing data, as expected, simulation studies have shown estimations remain unbiased[76,77]. Note, however, that although our approach took the uncertainty of missing data in the response or variable of interest (CT_{max}) into account, we used the most likely values for the predictors. While such an approach could underestimate the uncertainty in the response, point estimates should not be biased. In fact, our cross-validation approach demonstrated the ability of our models to predict back known experimental estimates with reasonable error (experimental mean ± standard deviation = 36.19 ± 2.67; imputed mean = 35.93 ± 2.54; r = 0.86; Extended Data Fig. 2).

Heat tolerance limits were imputed based on the species' acclimation temperatures, the duration of acclimation, the ramping rate and endpoint used in assays, the medium used for measuring heat tolerance limits (i.e., ambient temperatures, water/body temperatures), and the life stage of the animals (adults or larvae), and their ecotype. These variables were correlated with amphibian heat tolerance limits and were fitted as covariates in Bayesian linear mixed models. We also weighted heat tolerance estimates based on the inverse of their sampling variance, accounted for phylogenetic non-independence using a correlation matrix of phylogenetic relatedness, and fitted random intercepts for species-specific effects and phylogenetic effects, as well as their correlation with acclimation temperatures (i.e., random slopes). In other words, we modelled species-specific slopes (acclimation response ratio) and partitioned the variance among phylogenetic and non-phylogenetic effects. We imputed data for adult amphibians assuming they were acclimated to the median, 5^{th}, or 95^{th} percentile operative body temperatures experienced across their geographical range (see *Microenvironmental data and biophysical modelling)* for a duration of 10 days, tested using a ramping rate of 1°C/min in a container filled with water, and for which thermal tolerance endpoint was recorded as the onset of spasms. These methodological parameters were the median values in the experimental dataset, or the most common values (mode). This allowed standardization of heat tolerance limits for the comparative analysis[78–80]. In amphibians, the onset of spasms usually occurs after the loss of righting response[81], meaning that our estimates are conservative. While we did include data from larvae in the training data, we only imputed data for adults to increase the comparability of our estimates.

For both known species and data-deficient species, we generated three ecologically relevant and standardised heat tolerance estimates, and all analyses were built upon these standardised imputed

570 estimates. In total, we generated data for 5,203 species of amphibians (Extended Data Fig. 1-2). Notably,
571 our imputed estimates are accompanied by standard errors, which provide estimates of uncertainty in the
572 imputation, and errors were propagated throughout our analyses (see *Climate vulnerability analysis*).

573 ***Microenvironmental data and biophysical modelling***

574 We used the package *NicheMapR*[82,83] (v. 3.2.1) to estimate microenvironmental temperatures and hourly
575 operative body temperatures in current (2006-2015) and projected climatic conditions (2°C or 4°C of global
576 warming above pre-industrial levels). Operative body temperatures are the steady-state body temperatures
577 that organisms would achieve in a given microenvironment, which can diverge significantly from ambient
578 air temperatures due to, for example, radiative and evaporative heat exchange processes[19,20,84–89].

579 For each geographic location, we generated microclimatic temperatures experienced by amphibians on i) a
580 vegetated ground-level substrate (i.e., terrestrial), ii) in above-ground vegetation (i.e., arboreal), or iii) in a
581 water body (i.e., aquatic) (Extended Data Fig, 1). For terrestrial and aquatic species, we simulated
582 microenvironmental temperatures 1 cm above the surface. For arboreal species, we simulated
583 microenvironmental temperatures 2 meters above ground, applied a reduction of 80% in windspeed to
584 account for reduced wind due to vegetation[90], and assumed that 90% of the solar radiation was diffused due
585 to canopy cover[81]. All microenvironmental projections were made using 85% shade to simulate animals in
586 thermal refugia, i.e., the microhabitats in which animals would retreat during the hottest times of the day.
587 We did not model temperatures in the sun because ectothermic species most likely behaviourally
588 thermoregulate by retreating to thermal refugia during extreme heat events[21]. Our calculations thus
589 represent conservative estimates of the vulnerability of amphibians to extreme temperature events.

590 For microclimatic temperature estimates, we used the *micro_ncep* function from *NicheMapR*[82] (v. 3.2.1),
591 which integrates 6-hourly macroclimatic data from the National Center for Environmental Predictions
592 (NCEP). This function also inputs from the *microclima* package[92] (v. 0.1.0) to predict microclimatic
593 temperatures after accounting for variation in radiation, wind speed, altitude, albedo, vegetation, and
594 topography. These data are downscaled to an hourly resolution, producing high-resolution microclimatic
595 data. We used projected future monthly climate data from TerraClimate[23] to generate hourly projections

assuming 2°C or 4°C of global warming above pre-industrial levels. These temperatures are within the range projected by the end of the century under low (Shared Socioeconomic Pathway SSP 1-2.6 to SSP 2-4.5) and high (SSP 3-7.0 to SSP 5-8.5) greenhouse gas emission scenarios, respectively[24]. TerraClimate projections use monthly data on precipitation, minimum temperature, maximum temperature, wind speed, vapor pressure deficit, soil moisture, and downward surface shortwave radiation. These projections impose monthly climate projections from 23 CMIP5 global circulation models, as described in [93]. The *micro_ncep* function then downscales monthly TerraClimate inputs to hourly by imposing a diurnal cycle to the data and imposes TerraClimate offsets onto the climatic data from NCEP. Because the TerraClimate data is already bias-corrected, adding future climate projections onto the NCEP data did not require further bias correction. We ran all microclimatic estimations between 2005 and 2015 to match the range of pseudo-years available for TerraClimate future climate projections. We did not use a larger range of historical records and only used climate projections available in TerraClimate (i.e., 2°C and 4°C) to reduce computational demands.

We then used microclimate estimates to generate hourly operative body temperatures using the *ectotherm* function in *NicheMapR*[83]. This modelling system has been extensively validated with field observations[94–96] (*see also* Extended Data Fig. 10). We modelled an adult amphibian in the shape of the leopard frog *Lithobates pipiens*, positioned 1 cm above ground (or 2 m for arboreal species), and assumed that 80% of the skin acted as a free water surface (wet skin). Estimating body mass-specific operative body temperatures for each grid cell, species, and microhabitat was too computationally extensive, given the geographic and taxonomic scale of our study (464,871 local species occurrences). Therefore, we ran the ectotherm models using the median body mass of the species assemblage in each geographical coordinate. When body mass was unknown, we ran models assuming a body mass of 8.4 grams, the median assemblage-level body mass. Given that most amphibians in our dataset are small (median = 1.4 g, mean = 27.5 g), body temperatures equilibrate quickly with the environment, and operative body temperatures are likely representative of core body temperatures.

To model operative body temperatures in water bodies (e.g., ponds or wetlands), we used the container model from *NicheMapR*. Unlike previously mentioned calculations predicting steady-state temperatures,

this approach accounts for transient temperature changes, capturing lags due to thermal inertia (i.e., transient heat budget model[97,98]). For pond simulations, we modelled a container permanently filled with water (12 m width and 1.5 m-depth) and decreased direct solar radiation to zero to simulate full shade. This modelling approach serves as a proxy for estimating the body temperature of ectotherms submerged in water bodies such as ponds or wetlands, which was validated with field measurements (e.g., [40,95]). Ground-level and water temperatures were modelled for all species regardless of their ecotype (apart from paedomorphic salamanders that were only assessed in aquatic environments) because arboreal and terrestrial species may retreat on land or in water occasionally. Temperatures in above-ground vegetation were only estimated for arboreal and semi-arboreal species as reaching 2 meters height in vegetation requires a morphology adapted to climbing. Our biophysical models assume that shaded microhabitats are available to species throughout their range. While this may not hold true, fine-scaled distribution of these microenvironments are not available at global scales. Moreover, assuming that these microenvironments are available serves a functional role; it provides a best-case scenario that is useful for comparative analyses and offers actionable insights for conservation. For instance, reduced exposure to overheating events in aquatic relative to terrestrial environments would suggest that preserving ponds and wetlands may be critical in buffering the impacts of climate change on amphibians.

We then estimated, for each geographical coordinate, the maximum daily body temperature and the mean and maximum weekly maximum body temperature experienced in the 7 days prior to each given day to account for acclimation responses and to assess climate vulnerability metrics[18] (see *Climate vulnerability analyses*). We only used data for the 91 warmest days (i.e., warmest quarter) of each year, as we were interested in the responses of amphibians to extreme heat events[18]. Note that data from the year 2005 was excluded *a posteriori* as a burn-in to remove the effects of initial conditions on soil temperature, soil moisture, and pond calculations. Therefore, our analyses are based on 910 days (91 days per year in the range 2006-2015) for each climatic scenario (current climate, 2°C above pre-industrial levels, 4°C above pre-industrial levels).

We also used maximum daily body temperatures on terrestrial conditions to calculate the median, 5^{th} percentile and 95^{th} percentile maximum body temperature experienced by each species across their range

of distribution. These values were used as acclimation temperatures in the training data to calibrate the data imputation with ecologically-relevant environmental temperatures (see *Data imputation*); while maximizing the range of temperatures used to infer the plasticity of heat tolerance limits (see *Climate vulnerability analysis*).

Climate vulnerability analysis

Using the imputed data, we fitted an individual meta-analytic model for each species to estimate the plasticity of imputed heat tolerance limits (CT_{max}) to changes in operative body temperatures using the *metafor* package[99] (v. 4.2-0). CT_{max} was used as the response variable, acclimation temperature (i.e., median, 5th percentile, or 95th percentile daily maximum body temperature experienced by a species across its distribution range) was used as the predictor variable, and imputed estimates were weighted based on their standard error. From these models, we used out-of-sample model predictions (using the *predict* function) to estimate the CT_{max} of each species in each 1° x 1° grid cell across their distribution range in different warming scenarios, based on predicted mean weekly body temperatures. Specifically, we assumed that species were, on any given day, acclimated to the mean daily body temperature experienced in the 7 days prior[18]. Therefore, CT_{max} was simulated as a plastic trait, which varied daily, as animals acclimate to new environmental conditions (Extended Data Fig. 1). While evidence in small amphibians suggests the full acclimation potential is reached within 3-4 days[100–102], other evidence points to some variation after longer periods[103]. Therefore, we chose 7 days to reflect that some amphibians may require longer to acclimate. Because we used out-of-sample model predictions, we propagated errors from the imputation when estimating the predicted CT_{max} across geographical coordinates. Predicted CT_{max} values and their associated standard errors thus reflect variation in both the imputation procedure and the estimation of plastic responses. Our approach to accounting for plasticity assumes that plasticity is homogeneous within species and ignores the possible influence of local adaptation. However, given the low variability in plasticity among species (mean acclimation response ratio ± s.d. = 0.134 ± 0.008; range = 0.049 – 0.216; n = 5203), lack of evidence for latitudinal variation in plasticity ([28,31,104]), high phylogenetic signal in thermal tolerance (Pagel's λ[105] = 0.95 [0.91 – 0.98]; see *Sensitivity Analyses*), and evidence for slow rates of

evolution and physiological constraints on CT_{max}[52,53], geographic variation in thermal tolerance and plasticity is unlikely to have a major influence on our results.

We then estimated the vulnerability of amphibians to global warming using three metrics (Extended Data Fig. 1). First, we calculated the difference between CT_{max} and the maximum daily body temperature, i.e., the thermal safety margin (i.e., TSM, *sensu* [6]). We calculated weighted means and standard errors (*sensu* [106]) of thermal safety margins across years to estimate the mean difference between CT_{max} and the maximum temperature during the warmest quarters. Using TSM averaged from the maximum temperature of the warmest quarter is common in the literature[27–29]. Second, we calculated the number of days the maximum daily operative body temperature exceeded CT_{max} across the warmest quarters of 2006-2015, i.e., the number of overheating events. To propagate the uncertainty, we calculated the mean probability that daily operative body temperatures exceeded the predicted distribution of CT_{max} (using the *dnorm* function). Note that the standard error (standard deviation of estimates) of simulated CT_{max} distributions were restricted to one (i.e., simulating distributions within ~3°C of the mean) to avoid inflating overheating probabilities due to large imputation uncertainty (*cf* [75]*;* see also *Sensitivity analyses*; Extended Data Fig. 8). We then multiplied the mean overheating probability by the total number of simulated days (910) to estimate the number of overheating events and their associated standard error using properties of the binomial distribution. Third, we calculated the binary probability (0/1) that species overheat for at least one day across the 910 days surveyed (warmest quarters of 2006-2015). The latter two metrics provide a finer resolution than TSMs, as they capture daily temperature fluctuations and potential overheating events[18].

Macroecological patterns

The objective of this study was to characterise the vulnerability of amphibians to global warming. We investigated patterns at the level of local species occurrences (presence of a given species in a 1° x 1° grid cell based on IUCN data), allowing one to identify specific populations and species that may be more susceptible to heat stress and direct targeted research efforts. We also analysed data at the assemblage level, the species composition within a grid cell. In such case, we calculated the weighted mean and standard error of TSM (*sensu* [105]) across species in each grid cell. Assemblage-level analyses allow one to identify

areas containing a higher number of vulnerable species, offering actionable insights for broader-scale conservation initiatives.

We used the *gamm4* package[106] to fit generalised additive mixed models (GAMM) against latitude. For local species occurrences, we fitted latitude as a fixed factor, and nested genus and species identity as random terms to account for phylogenetic non-independence. Note that we did not include family as a random term because models failed at estimating higher taxonomic variation. While better methods exist to model phylogenetic patterns, generalised additive linear models do not allow for phylogenetic correlation matrices, and other functions such as *brms*[107] surpassed our computational time and memory limits. Nevertheless, imputed estimates already reflect variation due to phylogeny (see *Data imputation*), and phylogeny was further modelled when deriving mean estimates in each microhabitat and climatic scenario (see below). We fitted models using the three metrics as response variables independently: the thermal safety margin, overheating risk, and number of overheating events. The former was modelled using a Gaussian distribution of residuals, overheating risk was modelled using a binomial error structure, and the latter using a Poisson error structure. Note that overheating risks were rounded to integer values to fit a Poisson distribution. Thermal safety margin estimates were weighted by the inverse of their sampling variance to account for the uncertainty in the imputation and predictions across geographical coordinates. We fitted separate models for each climatic scenario (current climate, 2°C above preindustrial levels, 4°C above preindustrial levels) and microhabitat (terrestrial, aquatic, arboreal).

To investigate the mean TSM in each microhabitat and climatic scenario, we fitted models with the interaction between microhabitat and climatic scenario as a fixed effect using *MCMCglmm*[73] (v. 2.34) and flat, parameter-expanded priors. In these models, we weighted estimates based on the inverse of their sampling variance, species identity was fitted as a random effect, and we accounted for phylogenetic non-independence using a variance-covariance matrix of phylogenetic relatedness (calculated from the consensus tree of [26]). To investigate the overall overheating risk and number of overheating events in each condition, we attempted to fit models in *MCMCglmm* but these models failed to converge. Therefore, we fitted Poisson and binomial models using *lme4*[108] (v. 1.1-33) and nested genus, species, and observation as random terms. We used similar Poisson models to investigate the relationship between the number of

overheating events and thermal safety margins. While the mean estimates from these simpler models should be unbiased, estimate uncertainty is likely underestimated[109].

We also investigated patterns of climate vulnerability at the assemblage level. We calculated the weighted average of TSM and overheating risk in each 1-degree grid cell (14,091; 14,090; or 6,614 grid cells for terrestrial, aquatic, and arboreal species, respectively), and mapped patterns geographically. Averaging overheating risk effectively returned the proportion of species overheating in each coordinate; and we also calculated the number of species overheating in each grid cell. For assemblage-level models, we fitted Gaussian, binomial or Poisson models as described above, but without taxon-level random effects because these cannot be modelled at the assemblage level. All models were fitted without a contrast structure to estimate mean effects in each microhabitat and climatic scenario, and with two-sided contrasts to draw comparisons with current terrestrial conditions.

Cross-validation and sensitivity analyses

We assessed the accuracy of the data imputation procedure using a cross-validation approach. Specifically, we removed heat tolerance estimates for 5% of the species in the experimental data and 5% of the data-deficient species (maintaining the same proportion of missing data) and assessed how well experimental values could be predicted from the models. Of relevance, we only removed data that were comparable to the data that were imputed. That is, data from adult animals tested using a ramping rate of 1°C/min, and where thermal limits were recorded as the onset of spasms. While we could have trimmed any data entry in the experimental data, validation of the imputation performance can only be achieved by comparing comparable entries, and imputing data from species tested in unusual settings would naturally result in large errors. In total, we cross-validated experimental estimates for 77 species.

We investigated alternative ways to i) calculate thermal safety margins, ii) account for acclimation responses, and iii) control for prediction uncertainty (Extended Data Fig. 6-8). In our study, we projected CT_{max} estimates assuming animals were acclimated to the mean weekly temperature experienced prior to each day. We also assessed the climate vulnerability of amphibians assuming they were acclimated to weekly maximum body temperatures (*cf.* [18]), which reflects more conservative estimates (Extended Data

Fig. 7). We also calculated thermal safety margins as the difference between the maximum (or 95th percentile, *cf.* [4]) hourly body temperature experienced by each population and their predicted CT_{max} to investigate the consequences of averaging temperatures when calculating TSMs (Extended Data Fig. 6). To increase the comparability of our estimations with similar studies (*e.g.,* [4]), we also calculated climate vulnerability metrics more conservatively. Specifically, we excluded temperature data falling below the 5th percentile and above the 95th percentile body temperature for each population to mitigate the impact of outliers (Extended Data Fig. 6). However, extreme weather events, which are typically captured by these outlier values, are the very phenomena most likely to precipitate mortality events[16,17]. Omitting these outliers could therefore obscure the ecological significance of extreme temperatures, thereby underestimating true overheating risks. To estimate overheating probabilities, we calculated the mean daily probability that operative body temperatures exceeded the predicted distribution of CT_{max} and restricted the standard deviation of simulated distributions to one (i.e., within ~3°C of the mean) to avoid inflating overheating probability for observations with large uncertainty. We also provided alternative results (Extended Data Fig. 8) where the standard deviation of CT_{max} was restricted to the "*biological range*", i.e., the standard deviation of the distribution of all CT_{max} estimates across species (range = 1.84 – 2.17). We also provide a sensitivity analysis where overheating risk was positive only when the 95% confidence intervals of predicted overheating days did not overlap with zero (Extended Data Fig. 8).

We also investigated the influence of different parameters of our biophysical models (i.e., shade and burrow availability, height in above-ground vegetation, solar radiation, wind speed, pond depth) on predicted vulnerability risks (Extended Data Fig. 9). Specifically, we modelled the responses of the species at highest risk in terrestrial and aquatic conditions, *Noblella myrmecoides,* in its most vulnerable location (latitude, longitude = -9.5, -69.5). For terrestrial conditions, we modelled the response of amphibians with different body sizes (0.5, 4.28, or 50 grams), and with different levels of exposure to open habitat conditions. Specifically, we modelled an amphibian exposed to 50% of shade to simulate an open habitat lightly covered by vegetation, and inferred temperatures at different soil depths (2.5, 5, 10, 15, or 20 cm underground). For aquatic conditions, we adjusted pond depths to simulate a very shallow pond (50 cm) and compared it to deeper ponds (1.5- or 3-meters depth). For arboreal conditions, we modelled the

responses of *Pristimantis ockendeni*, in its most vulnerable location (-4.5, -71.5), and adjusted the height in above-ground vegetation (0.5, 2, or 5 meters), the percentage of radiation diffused by vegetation (50%, 75%, or 90% of radiation diffused), and the percentage of wind speed reduced by vegetation (0%, 50%, or 80% of wind speed reduced by vegetation). We did not estimate the influence of these parameters on all species and at all locations because of the scale of our study, but these results should provide insight into how varying microenvironmental features and biological characteristics may impact our general conclusions. Our results were generally robust to changes in model parameters, although amphibians are likely to experience more overheating events in open habitats[6,42] and shallow ponds, and lower risks in underground conditions[111] (Extended Data Fig. 9).

We also compared our predictions of operative body temperatures with field body temperature measurements. We extracted night-time (18:00 – 00:30) field body temperatures measured for 11 species of frogs in Mexico (21.48° N, -104.85° W; and 21.45° N, -105.03° W) between June and October of 2013 and 2015 from Table 1 of [111]. We chose this study because it provided the data and location of body temperature measurements, covered multiple species from different sites, and matched our study timeframe (2006-2015). We then compare these estimates with hourly operative body temperatures predicted in shaded terrestrial conditions at the same dates and time windows (Extended Data Fig. 10). We confirmed that predicted operative body temperatures were comparable to field body temperatures measured in some wild frogs (Extended Data Fig. 10), and we invite additional validations with other species in different geographical areas.

Finally, we confirmed the presence of a phylogenetic signal in the experimental dataset by fitting a Bayesian linear mixed model using all complete (no missing data) predictors (i.e., acclimation temperature, endpoint, acclimation status, life stage, and ecotype) in *MCMCglmm*. We accounted for phylogenetic non-independence using a correlation matrix of phylogenetic relatedness and fitted random intercepts for non-phylogenetic species effects. The phylogenetic signal (Pagel's λ[105], which is equivalent to phylogenetic heritability[112,113]) was calculated as the proportion of variance explained by phylogenetic effects relative to the total non-residual variance.

Results from all statistical models and additional data visualizations are available at https://p-pottier.github.io/Vulnerability_amphibians_global_warming/.

Data availability

Raw and processed data are available at https://github.com/p-pottier/Vulnerability_amphibians_global_warming, and archived permanently in Zenodo[114]. Note, however, that some intermediate data files were too large to be shared online. These files are available upon request. TerraClimate data is available from https://www.climatologylab.org/terraclimate.html and NCEP data is available from https://psl.noaa.gov/thredds/catalog/Datasets/ncep.reanalysis2/gaussian_grid/catalog.html.

Code availability

All code needed to reproduce the analyses is available at https://github.com/p-pottier/Vulnerability_amphibians_global_warming, and archived permanently in Zenodo[114].

Methods references

61. McNutt, M. K. *et al.* Transparency in authors' contributions and responsibilities to promote integrity in scientific publication. *Proc. Natl. Acad. Sci. U.S.A.* **115**, 2557–2560 (2018).
62. Nakagawa, S. *et al.* Method Reporting with Initials for Transparency (MeRIT) promotes more granularity and accountability for author contributions. *Nat. Commun.* **14**, 1788 (2023).
63. Pottier, P. *et al.* Title, abstract and keywords: a practical guide to maximise the visibility and impact of academic papers. *Proc. R. Soc. B* **291**, 2023.10.02.559861 (2024).
64. R Core Team. R: A language and environment for statistical computing. R Foundation for Statistical Computing (2019).
65. South, A., Michael, S. & Massicotte, P. *rnaturalearthhires*: High resolution world vector map data from Natural Earth used in rnaturalearth. R package version 0.2.1. (2022).
66. Yu, G., Smith, D. K., Zhu, H., Guan, Y. & Lam, T. T. Y. ggtree: an R package for visualization and annotation of phylogenetic trees with their covariates and other associated data. *Methods Ecol. Evol.* 8, 28–36 (2017).
67. Wickham, H. *ggplot2*: Elegant graphics for data analysis. R package version 3.5.1. (2011).
68. Lutterschmidt, W. I. & Hutchison, V. H. The critical thermal maximum: history and critique. *Can. J. Zool.* **75**, 1561–1574 (1997).
69. IUCN. *The IUCN Red List of Threatened Species*. https://www.iucnredlist.org (2021).
70. Johnson, J. V. *et al.* What drives the evolution of body size in ectotherms? A global analysis across the amphibian tree of life. *Glob. Ecol. Biogeogr.* **32**, 1311–1322 (2023).
71. Santini, L., Benítez-López, A., Ficetola, G. F. & Huijbregts, M. A. J. Length–mass allometries in amphibians. *Integr. Zool.* **13**, 36–45 (2018).
72. Buuren, S. van & Groothuis-Oudshoorn, K. mice: Multivariate Imputation by Chained Equations in R. *J. Stat. Softw.* **45**, 1–67 (2011).
73. Hadfield, J. D. MCMC Methods for Multi-Response Generalized Linear Mixed Models: The MCMCglmm R Package. *J. Stat. Softw.* **33**, 1–22 (2010).
74. Speidel, M., Drechsler, J. & Jolani, S. *R Package Hmi: A Convenient Tool for Hierarchical Multiple Imputation and Beyond*. https://www.econstor.eu/handle/10419/182156 (2018).
75. Callaghan, C. T., Nakagawa, S. & Cornwell, W. K. Global abundance estimates for 9,700 bird species. *Proc. Natl. Acad. Sci. U.S.A.* **118**, e2023170118 (2021).
76. Austin, P. C. & van Buuren, S. The effect of high prevalence of missing data on estimation of the coefficients of a logistic regression model when using multiple imputation. *BMC Med. Res. Methodol.* **22**, 196 (2022).
77. Madley-Dowd, P., Hughes, R., Tilling, K. & Heron, J. The proportion of missing data should not be used to guide decisions on multiple imputation. *J. Clin. Epidemiol.* **110**, 63–73 (2019).

78. Lutterschmidt, W. I. & Hutchison, V. H. The critical thermal maximum: data to support the onset of spasms as the definitive end point. *Can. J. Zool.* **75**, 1553–1560 (1997).
79. Camacho, A. & Rusch, T. W. Methods and pitfalls of measuring thermal preference and tolerance in lizards. *J. Therm. Biol.* **68**, 63–72 (2017).
80. Hoffmann, A. A. & Sgrò, C. M. Comparative studies of critical physiological limits and vulnerability to environmental extremes in small ectotherms: How much environmental control is needed? *Integr. Zool.* **13**, 355–371 (2018).
81. Lutterschmidt, W. I. & Hutchison, V. H. The critical thermal maximum: data to support the onset of spasms as the definitive end point. *Can. J. Zool.* **75**, 1553–1560 (1997).
82. Kearney, M. R. & Porter, W. P. NicheMapR – an R package for biophysical modelling: the microclimate model. *Ecography* **40**, 664–674 (2017).
83. Kearney, M. R. & Porter, W. P. NicheMapR – an R package for biophysical modelling: the ectotherm and Dynamic Energy Budget models. *Ecography* **43**, 85–96 (2020).
84. Pincebourde, S. & Suppo, C. The Vulnerability of Tropical Ectotherms to Warming Is Modulated by the Microclimatic Heterogeneity. *Integr. Comp. Biol.* **56**, 85–97 (2016).
85. Tracy, C. R., Christian, K. A. & Tracy, C. R. Not just small, wet, and cold: effects of body size and skin resistance on thermoregulation and arboreality of frogs. *Ecology* **91**, 1477–1484 (2010).
86. Köhler, A. *et al.* Staying warm or moist? Operative temperature and thermal preferences of common frogs (Rana temporaria), and effects on locomotion. *Herpetol. J.* **21**, 17–26 (2011).
87. Navas, C. A., Carvajalino-Fernández, J. M., Saboyá-Acosta, L. P., Rueda-Solano, L. A. & Carvajalino-Fernández, M. A. The body temperature of active amphibians along a tropical elevation gradient: patterns of mean and variance and inference from environmental data. *Funct. Ecol.* **27**, 1145–1154 (2013).
88. Barton, M. G., Clusella-Trullas, S. & Terblanche, J. S. Spatial scale, topography and thermoregulatory behaviour interact when modelling species' thermal niches. *Ecography* **42**, 376–389 (2019).
89. García-García, A. *et al.* Soil heat extremes can outpace air temperature extremes. *Nat. Clim. Change* **13**, 1237–1241 (2023).
90. Davies-Colley, R. J., Payne, G. W. & van Elswijk, M. Microclimate gradients across a forest edge. *N. Z. J. Ecol.* **24**, 111–121 (2000).
91. Campbell, G. S. & Norman, J. M. *An Introduction to Environmental Biophysics*. (Springer Science & Business Media, 2000).
92. Maclean, I. M. D., Mosedale, J. R. & Bennie, J. J. Microclima: An r package for modelling meso- and microclimate. *Methods Ecol. Evol.* **10**, 280–290 (2019).
93. Qin, Y. *et al.* Agricultural risks from changing snowmelt. *Nat. Clim. Change* **10**, 459–465 (2020).
94. Tracy, C. R. A Model of the Dynamic Exchanges of Water and Energy between a Terrestrial Amphibian and Its Environment. *Ecol. Monogr.* **46**, 293–326 (1976).

95. Enriquez-Urzelai, U., Kearney, M. R., Nicieza, A. G. & Tingley, R. Integrating mechanistic and correlative niche models to unravel range-limiting processes in a temperate amphibian. *Glob. Change Biol.* **25**, 2633–2647 (2019).
96. Kearney, M. R., Munns, S. L., Moore, D., Malishev, M. & Bull, C. M. Field tests of a general ectotherm niche model show how water can limit lizard activity and distribution. *Ecol. Monogr.* **88**, 672–693 (2018).
97. Kearney, M. R., Porter, W. P. & Huey, R. B. Modelling the joint effects of body size and microclimate on heat budgets and foraging opportunities of ectotherms. *Methods Ecol. Evol.* **12**, 458–467 (2021).
98. Kearney, M. *et al.* Modelling species distributions without using species distributions: the cane toad in Australia under current and future climates. *Ecography* **31**, 423–434 (2008).
99. Viechtbauer, W. Conducting meta-analyses in R with the metafor package. *J. Stat. Softw.* **36**, 1–48 (2010).
100. Brattstrom, B. H. & Lawrence, P. The Rate of Thermal Acclimation in Anuran Amphibians. *Physiol. Zool.* **35**, 148–156 (1962).
101. Layne, J. R. & Claussen, D. L. The time courses of CTMax and CTMin acclimation in the salamander *Desmognathus fuscus*. *J. Therm. Biol.* **7**, 139–141 (1982).
102. Turriago, J. L., Tejedo, M., Hoyos, J. M., Camacho, A. & Bernal, M. H. The time course of acclimation of critical thermal maxima is modulated by the magnitude of temperature change and thermal daily fluctuations. *J. Therm. Biol.* **114**, 103545 (2023).
103. Dallas, J. & Warne, R. W. Heat hardening of a larval amphibian is dependent on acclimation period and temperature. *J. Exp. Zool. Part A* **339**, 339–345 (2023).
104. Ruthsatz, K. *et al.* Acclimation capacity to global warming of amphibians and freshwater fishes: Drivers, patterns, and data limitations. *Glob. Change Biol.* **30**, e17318 (2024).
105. Higgins, J. P. T. & Thompson, S. G. Quantifying heterogeneity in a meta-analysis. *Stat. Med.* **21**, 1539–1558 (2002).
106. Wood, S. & Scheipl, F. gamm4: Generalized additive mixed models using mgcv and lme4. (2014).
107. Bürkner, P.-C. brms: An R Package for Bayesian Multilevel Models Using Stan. *J. Stat. Softw.* **80**, 1–28 (2017).
108. Bates, D., Mächler, M., Bolker, B. & Walker, S. Fitting Linear Mixed-Effects Models using lme4. Preprint at https://doi.org/10.48550/arXiv.1406.5823 (2014).
109. Cinar, O., Nakagawa, S. & Viechtbauer, W. Phylogenetic multilevel meta-analysis: A simulation study on the importance of modelling the phylogeny. *Methods Ecol. Evol.* **13**, 383–395 (2022).
110. Carlo, M. A., Riddell, E. A., Levy, O. & Sears, M. W. Recurrent sublethal warming reduces embryonic survival, inhibits juvenile growth, and alters species distribution projections under climate change. *Ecol. Lett.* **21**, 104–116 (2018).

111. Lara-Resendiz, R. A., & Luja, V. H. Body temperatures of some amphibians from Nayarit, Mexico. *Rev. Mex. Biodivers.* **89**, 577-581 (2018).
112. Hadfield, J. D. & Nakagawa, S. General quantitative genetic methods for comparative biology: phylogenies, taxonomies and multi-trait models for continuous and categorical characters. *J. Evol. Biol.* **23**, 494–508 (2010).
113. Lynch, M. Methods for the Analysis of Comparative Data in Evolutionary Biology. *Evolution* **45**, 1065–1080 (1991).
114. Pottier, P. *et al.* Data and code for: Vulnerability of amphibians to global warming. *Zenodo*. version 1.0.0. https://doi.org/10.5281/zenodo.14498866 (2024).
115. Ivimey-Cook, E. R. *et al.* Implementing code review in the scientific workflow: Insights from ecology and evolutionary biology. *J. Evol. Biol.* **36**, 1347–1356 (2023).
116. Agudelo-Cantero, G. A. & Navas, C. A. Interactive effects of experimental heating rates, ontogeny and body mass on the upper thermal limits of anuran larvae. *J. Therm. Biol.* **82**, 43–51 (2019).
117. Alveal Riquelme, N. *Relaciones entre la fisiología térmica y las características bioclimáticas de Rhinella spinulosa (Anura: Bufonidae) en Chile a través del enlace mecanicista de nicho térmico* (Universidad de Concepción, 2015).
118. Alves, M. *Tolerância térmica em espécies de anuros neotropicais do gênero Dendropsophus Fitzinger, 1843 e efeito da temperatura na resposta à predação* (Universidade Estadual de Santa Cruz, 2016).
119. Anderson, R. C. O. & Andrade, D. V. Trading heat and hops for water: Dehydration effects on locomotor performance, thermal limits, and thermoregulatory behavior of a terrestrial toad. *Ecol. Evol.* **7**, 9066–9075 (2017).
120. Aponte Gutiérrez, A. *Endurecimiento térmico en Pristimantis medemi (Anura: Craugastoridae), en coberturas boscosas del Municipio de Villavicencio (Meta)* (Universidad Nacional de Colombia, 2020).
121. Arrigada García, K. *Conductas térmica en dos poblaciones de Batrachyla taeniata provenientes de la localidad de Ucúquer en la región de O'Higgins y de la localidad de Hualpén en la región del Bío-Bío* (Universidad de Concepción, 2019).
122. Azambuja, G., Martins, I. K., Franco, J. L. & Santos, T. G. dos. Effects of mancozeb on heat Shock protein 70 (HSP70) and its relationship with the thermal physiology of Physalaemus henselii (Peters, 1872) tadpoles (Anura: Leptodactylidae). *J. Therm. Biol.* **98**, 102911 (2021).
123. Bacigalupe, L. D. *et al.* Natural selection on plasticity of thermal traits in a highly seasonal environment. *Evol. Appl.* **11**, 2004–2013 (2018).
124. Barria, A. M. & Bacigalupe, L. D. Intraspecific geographic variation in thermal limits and acclimatory capacity in a wide distributed endemic frog. *J. Therm. Biol.* **69**, 254–260 (2017).

125. Beltrán, I., Ramírez-Castañeda, V., Rodríguez-López, C., Lasso, E. & Amézquita, A. Dealing with hot rocky environments: critical thermal maxima and locomotor performance in Leptodactylus lithonaetes (Anura: Leptodactylidae). *Herpetol. J.* **29**, 155–161 (2019).
126. Berkhouse, C. & Fries, J. Critical thermal maxima of juvenile and adult San Marcos salamanders (Eurycea nana). *Southwest. Nat.* **40**, 430–434 (1995).
127. Blem, C. R., Ragan, C. A. & Scott, L. S. The thermal physiology of two sympatric treefrogs Hyla cinerea and Hyla chrysoscelis (Anura; Hylidae). *Comp. Biochem. Physiol. A Physiol.* **85**, 563–570 (1986).
128. Bonino, M. F., Cruz, F. B. & Perotti, M. G. Does temperature at local scale explain thermal biology patterns of temperate tadpoles? *J. Therm. Biol.* **94**, (2020).
129. Bovo, R. P. *Fisiologia térmica e balanço hídrico em anfíbios anuros* (Universidad Estadual Paulista, 2015).
130. Brattstrom, B. H. Thermal acclimation in Australian amphibians. *Comp. Biochem. Physiol.* **35**, 69–103 (1970).
131. Brattstrom, B. H. & Regal, P. Rate of thermal acclimation in the Mexican salamander Chiropterotriton. *Copeia* **1965**, 514–515 (1965).
132. Brattstrom, B. H. A preliminary review of the thermal requirements of amphibians. *Ecology* **44**, 238–255 (1963).
133. Brattstrom, B. H. Thermal acclimation in anuran amphibians as a function of latitude and altitude. *Comp. Biochem. Physiol.* **24**, 93–111 (1968).
134. Brattstrom, B. H. & Lawrence, P. The rate of thermal acclimation in anuran amphibians. *Physiol. Zool.* **35**, 148–156 (1962).
135. Brown, H. A. The heat resistance of some anuran tadpoles (Hylidae and Pelobatidae). *Copeia* **1969**, 138 (1969).
136. Burke, E. M. & Pough, F. H. The role of fatigue in temperature resistance of salamanders. *J. Therm. Biol.* **1**, 163–167 (1976).
137. Burrowes, P. A., Navas, C. A., Jiménez-Robles, O., Delgado, P. & De La Riva, I. Climatic heterogeneity in the Bolivian Andes: Are frogs trapped? *South Am. J. Herpetol.* **18**, 1–12 (2020).
138. Bury, R. B. Low thermal tolerances of stream amphibians in the Pacific Northwest: Implications for riparian and forest management. *Appl. Herpetol.* **5**, 63–74 (2008).
139. Castellanos García, L. A. *Days of futures past: integrating physiology, microenvironments, and biogeographic history to predict response of frogs in neotropical dry-forest to global warming* (Universidad de los Andes, 2017).
140. Castro, B. *Influence of environment on thermal ecology of direct-developing frogs (Anura: Craugastoridae: Pristimantis) in the eastern Andes of Colombia* (Universidad de los Andes, 2019).
141. Catenazzi, A., Lehr, E. & Vredenburg, V. T. Thermal physiology, disease, and amphibian declines on the eastern slopes of the Andes. *Conserv. Biol.* **28**, 509–517 (2014).

142. Chang, L.-W. *Heat tolerance and its plasticity in larval Bufo bankorensis from different altitudes* (National Cheng Kung University, 2002).
143. Chavez Landi, P. A. *Fisiología térmica de un depredador Dasythemis sp.(Odonata: Libellulidae) y su presa Hypsiboas pellucens (Anura: Hylidae) y sus posibles implicaciones frente al cambio climático* (Pontificia Universidad Católica Del Ecuador, 2017).
144. Chen, T.-C., Kam, Y.-C. & Lin, Y.-S. Thermal physiology and reproductive phenology of Buergeria japonica (Rhacophoridae) breeding in a stream and a geothermal hotspring in Taiwan. *Zool. Sci.* **18**, 591–596 (2001).
145. Cheng, C.-B. *A study of warming tolerance and thermal acclimation capacity of tadpoles in Taiwan* (Tunghai University, 2017).
146. Cheng, Y.-J. *Effect of salinity on the critical thermal maximum of tadpoles living in brackish water* (Tunghai University, 2017).
147. Christian, K. A., Nunez, F., Clos, L. & Diaz, L. Thermal relations of some tropical frogs along an altitudinal gradient. *Biotropica* **20**, 236–239 (1988).
148. Claussen, D. L. The thermal relations of the tailed frog, Ascaphus truei, and the Pacific treefrog, Hyla regilla. *Comp. Biochem. Physiol. A Physiol.* **44**, 137–153 (1973).
149. Claussen, D. L. Thermal acclimation in ambystomatid salamanders. *Comp. Biochem. Physiol. A Physiol.* **58**, 333–340 (1977).
150. Contreras Cisneros, J. *Temperatura crítica máxima, tolerancia al frío y termopreferendum del tritón del Montseny (Calotriton arnoldii)* (Universitat de Barcelona, 2019).
151. Contreras Oñate, S. *Posible efecto de las temperaturas de aclimatación sobre las respuestas térmicas en temperaturas críticas máximas (TCmás) y mínimas (TCmín) de una población de Batrachyla taeniata (Girard, 1955)* (Universidad de Concepción, 2016).
152. Cooper, R. D. & Shaffer, H. B. Allele-specific expression and gene regulation help explain transgressive thermal tolerance in non-native hybrids of the endangered California tiger salamander (Ambystoma californiense). *Mol. Ecol.* **30**, 987–1004 (2021).
153. Crow, J. C., Forstner, M. R. J., Ostr, K. G. & Tomasso, J. R. The role of temperature on survival and growth of the Barton Springs salamander (Eurycea sosorum). *Herpetol. Conserv. Biol.* **11**, 328–334 (2016).
154. Cupp, P. V. Thermal tolerance of five salientian amphibians during development and metamorphosis. *Herpetologica* **36**, 234–244 (1980).
155. Dabruzzi, T. F., Wygoda, M. L. & Bennett, W. A. Some like it hot: Heat tolerance of the crab-eating frog, Fejervarya cancrivora. *Micronesica* **43**, 101–106 (2012).
156. Dainton, B. H. Heat tolerance and thyroid activity in developing tadpoles and juvenile adults of Xenopus laevis (Daudin). *J. Therm. Biol.* **16**, 273–276 (1991).
157. Daniel, N. J. J. *Impact of climate change on Singapore amphibians* (National University of Singapore, 2013).

158. Davies, S. J., McGeoch, M. A. & Clusella-Trullas, S. Plasticity of thermal tolerance and metabolism but not water loss in an invasive reed frog. *Comp. Biochem. Physiol. A Mol. Integr. Physiol.* **189**, 11–20 (2015).
159. de Oliviera Anderson, R. C., Bovo, R. P. & Andrade, D. V. Seasonal variation in the thermal biology of a terrestrial toad, Rhinella icterica (Bufonidae), from the Brazilian Atlantic Forest. *J. Therm. Biol.* **74**, 77–83 (2018).
160. de Vlaming, V. L. & Bury, R. B. Thermal selection in tadpoles of the tailed-frog, Ascaphus truei. *J. Herpetol.* **4**, 179–189 (1970).
161. Delson, J. & Whitford, W. G. Critical thermal maxima in several life history stages in desert and montane populations of Ambystoma tigrinum. *Herpetologica* **29**, 352–355 (1973).
162. Duarte, H. *et al*. Can amphibians take the heat? Vulnerability to climate warming in subtropical and temperate larval amphibian communities. *Glob. Change Biol.* **18**, 412–421 (2012).
163. Duarte, H. S. *A comparative study of the thermal tolerance of tadpoles of Iberian anurans* (Universidade de Lisboa, 2011).
164. Dunlap, D. Evidence for a daily rhythm of heat resistance in cricket frogs, Acris crepitans. *Copeia* **1969**, 852– (1969).
165. Dunlap, D. G. Critical thermal maximum as a function of temperature of acclimation in two species of Hylid frogs. *Physiol. Zool.* **41**, 432–439 (1968).
166. Elwood, J. R. L. *Variation in hsp70 levels and thermotolerance among terrestrial salamanders of the Plethodon glutinosus complex* (Drexel University, 2003).
167. Enriquez-Urzelai, U. *et al*. Ontogenetic reduction in thermal tolerance is not alleviated by earlier developmental acclimation in Rana temporaria. *Oecologia* **189**, 385–394 (2019).
168. Enriquez-Urzelai, U. *et al*. The roles of acclimation and behaviour in buffering climate change impacts along elevational gradients. *J. Anim. Ecol.* **89**, 1722–1734 (2020).
169. Erskine, D. J. & Hutchison, V. H. Reduced thermal tolerance in an amphibian treated with melatonin. *J. Therm. Biol.* **7**, 121–123 (1982).
170. Escobar Serrano, D. *Acclimation scope of the critical thermal limits in Agalychnis spurrelli (Hylidae) and Gastrotheca pseustes (Hemiphractidae) and their implications under climate change scenarios* (Pontificia Universidad Católica Del Ecuador, 2016).
171. Fan, X., Lei, H. & Lin, Z. Ontogenetic shifts in selected body temperature and thermal tolerance of the tiger frog, Hoplobatrachus chinensis. *Acta Ecol. Sin.* **32**, 5574–5580 (2012).
172. Fan, X. L., Lin, Z. H. & Scheffers, B. R. Physiological, developmental, and behavioral plasticity in response to thermal acclimation. *J. Therm. Biol.* **97**, (2021).
173. Fernández-Loras, A. *et al.* Infection with Batrachochytrium dendrobatidis lowers heat tolerance of tadpole hosts and cannot be cleared by brief exposure to CTmax. *PLoS ONE* **14**, (2019).
174. Floyd, R. B. Ontogenetic change in the temperature tolerance of larval Bufo marinus (Anura: Bufonidae). *Comp. Biochem. Physiol. A Physiol.* **75**, 267–271 (1983).

175. Floyd, R. B. Effects of photoperiod and starvation on the temperature tolerance of larvae of the giant toad, Bufo marinus. *Copeia* **1985**, 625–631 (1985).
176. Fong, S.-T. *Thermal tolerance of adult Asiatic painted frog Kaloula pulchra from different populations* (National University of Tainan, 2014).
177. Frishkoff, L. O., Hadly, E. A. & Daily, G. C. Thermal niche predicts tolerance to habitat conversion in tropical amphibians and reptiles. *Glob. Change Biol.* **21**, 3901–3916 (2015).
178. Frost, J. S. & Martin, E. W. A comparison of distribution and high temperature tolerance in Bufo americanus and Bufo woodhousii fowleri. *Copeia* **1971**, 750 (1971).
179. Gatz, A. J. Critical thermal maxima of Ambystoma maculatum (Shaw) and Ambystoma jeffersonianum (Green) in relation to time of breeding. *Herpetologica* **27**, 157–160 (1971).
180. Gatz, A. J. Intraspecific variations in critical thermal maxima of Ambystoma maculatum. *Herpetologica* **29**, 264–268 (1973).
181. Geise, W. & Linsenmair, K. E. Adaptations of the reed frog Hyperolius viridiflavus to its arid environment - IV. Oecological significance of water economy with comments on thermoregulation and energy allocation. *Oecologia* **77**, 327–338 (1988).
182. González-del-Pliego, P. *et al.* Thermal tolerance and the importance of microhabitats for Andean frogs in the context of land use and climate change. *J. Anim. Ecol.* **89**, 2451–2460 (2020).
183. Gouveia, S. F. *et al.* Climatic niche at physiological and macroecological scales: The thermal tolerance–geographical range interface and niche dimensionality. *Glob. Ecol. Biogeogr.* **23**, 446–456 (2014).
184. Gray, R. Lack of physiological differentiation in three color morphs of the cricket frog (Acris crepitans) in Illinois. *Trans. Ill. State Acad. Sci.* **70**, 73–79 (1977).
185. Greenspan, S. E. *et al.* Infection increases vulnerability to climate change via effects on host thermal tolerance. *Sci. Rep.* **7**, (2017).
186. Guevara-Molina, E. C., Gomes, F. R. & Camacho, A. Effects of dehydration on thermoregulatory behavior and thermal tolerance limits of Rana catesbeiana (Shaw, 1802). *J. Therm. Biol.* **93**, (2020).
187. Gutiérrez Pesquera, L. *Una valoración macrofisiológica de la vulnerabilidad al calentamiento global. Análisis de los límites de tolerancia térmica en comunidades de anfibios en gradientes latitudinales y altitudinales* (Pontificia Universidad Católica Del Ecuador, 2015).
188. Gutiérrez Pesquera, M. *Thermal tolerance across latitudinal and altitudinal gradients in tadpoles* (Universidad de Sevilla, 2016).
189. Gutiérrez-Pesquera, L. M. *et al.* Testing the climate variability hypothesis in thermal tolerance limits of tropical and temperate tadpoles. *J. Biogeogr.* **43**, 1166–1178 (2016).
190. Gvoždík, L., Puky, M. & Šugerková, M. Acclimation is beneficial at extreme test temperatures in the Danube crested newt, Triturus dobrogicus (Caudata, Salamandridae). *Biol. J. Linn. Soc.* **90**, 627–636 (2007).

191. Heatwole, H., De Austin, S. B. & Herrero, R. Heat tolerances of tadpoles of two species of tropical anurans. *Comp. Biochem. Physiol.* **27**, 807–815 (1968).
192. Heatwole, H., Mercado, N. & Ortiz, E. Comparison of critical thermal maxima of two species of Puerto Rican frogs of the genus Eleutherodactylus. *Physiol. Zool.* **38**, 1–8 (1965).
193. Holzman, N. & McManus, J. J. Effects of acclimation on metabolic rate and thermal tolerance in the carpenter frog, Rana vergatipes. *Comp. Biochem. Physiol. A Physiol.* **45**, 833–842 (1973).
194. Hoppe, D. M. Thermal tolerance in tadpoles of the chorus frog Pseudacris triseriata. *Herpetologica* **34**, 318–321 (1978).
195. Hou, P.-C. *Thermal tolerance and preference in the adult amphibians from different altitudinal LTER sites* (National Cheng Kung University, 2003).
196. Howard, J. H., Wallace, R. L. & Stauffer Jr, J. R. Critical thermal maxima in populations of Ambystoma macrodactylum from different elevations. *J. Herpetol.* **17**, 400–402 (1983).
197. Hutchison, V. H. & Ritchart, J. P. Annual cycle of thermal tolerance in the salamander, Necturus maculosus. *J. Herpetol.* **23**, 73–76 (1989).
198. Hutchison, V. H. The distribution and ecology of the cave salamander, Eurycea lucifuga. *Ecol. Monogr.* **28**, 2–20 (1958).
199. Hutchison, V. H. Critical thermal maxima in salamanders. *Physiol. Zool.* **34**, 92–125 (1961).
200. Hutchison, V. H., Engbretson, G. & Turney, D. Thermal acclimation and tolerance in the hellbender, Cryptobranchus alleganiensis. *Copeia* **1973**, 805–807 (1973).
201. Hutchison, V. H. & Rowlan, S. D. Thermal acclimation and tolerance in the mudpuppy, Necturus maculosus. *J. Herpetol.* **9**, 367–368 (1975).
202. Jiang, S., Yu, P. & Hu, Q. A study on the critical thermal maxima of five species of salamanders of China. *Acta Herpetol. Sin.* **6**, 56–62 (1987).
203. John-Alder, H. B., Morin, P. J. & Lawler, S. Thermal physiology, phenology, and distribution of tree frogs. *Am. Nat.* **132**, 506–520 (1988).
204. Johnson, C. R. Daily variation in the thermal tolerance of Litoria caerulea (Anura: Hylidae). *Comp. Biochem. Physiol. A Physiol.* **40**, 1109–1111 (1971).
205. Johnson, C. R. Thermal relations and water balance in the day frog, Taudactylus diurnus, from an Australian rain forest. *Aust. J. Zool.* **19**, 35–39 (1971).
206. Johnson, C. R. Diel variation in the thermal tolerance of Litoria gracilenta (Anura: Hylidae). *Comp. Biochem. Physiol. A Physiol.* **41**, 727–730 (1972).
207. Johnson, C. R. & Prine, J. E. The effects of sublethal concentrations of organophosphorus insecticides and an insect growth regulator on temperature tolerance in hydrated and dehydrated juvenile western toads, Bufo boreas. *Comp. Biochem. Physiol. A Physiol.* **53**, 147–149 (1976).
208. Johnson, C. R. Observations on body temperatures, critical thermal maxima and tolerance to water loss in the Australian hylid, Hyla caerulea (White). *Proc. R. Soc. Qld.* **82**, 47–50 (1970).

209. Johnson, C. R. Thermal relations and daily variation in the thermal tolerance in Bufo marinus. *J. Herpetol.* **6**, 35 (1972).
210. Johnson, C. Thermal relations in some southern and eastern Australian anurans. *Proc. R. Soc. Qld.* **82**, 87–94 (1971).
211. Johnson, C. The effects of five organophosphorus insecticides on thermal stress in tadpoles of the Pacific tree frog, Hyla regilla. *Zool. J. Linn. Soc.* **69**, 143–147 (1980).
212. Katzenberger, M., Duarte, H., Relyea, R., Beltrán, J. F. & Tejedo, M. Variation in upper thermal tolerance among 19 species from temperate wetlands. *J. Therm. Biol.* **96**, (2021).
213. Katzenberger, M. *et al.* Swimming with predators and pesticides: How environmental stressors affect the thermal physiology of tadpoles. *PLoS ONE* **9**, (2014).
214. Katzenberger, M., Hammond, J., Tejedo, M. & Relyea, R. Source of environmental data and warming tolerance estimation in six species of North American larval anurans. *J. Therm. Biol.* **76**, 171–178 (2018).
215. Katzenberger, M. *Thermal tolerance and sensitivity of amphibian larvae from Palearctic and Neotropical communities* (Universidade de Lisboa, 2013).
216. Katzenberger, M. *Impact of global warming in Holarctic and Neotropical communities of amphibians* (Universidad de Sevilla, 2014).
217. Kern, P., Cramp, R. L. & Franklin, C. E. Temperature and UV-B-insensitive performance in tadpoles of the ornate burrowing frog: An ephemeral pond specialist. *J. Exp. Biol.* **217**, 1246–1252 (2014).
218. Kern, P., Cramp, R. L., Seebacher, F., Ghanizadeh Kazerouni, E. & Franklin, C. E. Plasticity of protective mechanisms only partially explains interactive effects of temperature and UVR on upper thermal limits. *Comp. Biochem. Physiol. A Mol. Integr. Physiol.* **190**, 75–82 (2015).
219. Kern, P., Cramp, R. L. & Franklin, C. E. Physiological responses of ectotherms to daily temperature variation. *J. Exp. Biol.* **218**, 3068–3076 (2015).
220. Komaki, S., Igawa, T., Lin, S.-M. & Sumida, M. Salinity and thermal tolerance of Japanese stream tree frog (Buergeria japonica) tadpoles from island populations. *Herpetol. J.* **26**, 207–211 (2016).
221. Komaki, S., Lau, Q. & Igawa, T. Living in a Japanese onsen: Field observations and physiological measurements of hot spring amphibian tadpoles, Buergeria japonica. *Amphibia-Reptilia* **37**, 311–314 (2016).
222. Krakauer, T. Tolerance limits of the toad, Bufo marinus, in South Florida. *Comp. Biochem. Physiol.* **33**, 15–26 (1970).
223. Kurabayashi, A. *et al.* Improved transport of the model amphibian, Xenopus tropicalis, and its viable temperature for transport. *Curr. Herpetol.* **33**, 75–87 (2014).
224. Lau, E. T. C., Leung, K. M. Y. & Karraker, N. E. Native amphibian larvae exhibit higher upper thermal limits but lower performance than their introduced predator Gambusia affinis. *J. Therm. Biol.* **81**, 154–161 (2019).

225. Layne, J. R. & Claussen, D. L. Seasonal variation in the thermal acclimation of critical thermal maxima (CTMax) and minima (CTMin) in the salamander Eurycea bislineata. *J. Therm. Biol.* **7**, 29–33 (1982).
226. Layne, J. R. & Claussen, D. L. The time courses of CTMax and CTMin acclimation in the salamander Desmognathus fuscus. *J. Therm. Biol.* **7**, 139–141 (1982).
227. Lee, P.-T. *Acidic effect on tadpoles living in container habitats* (Tunghai University, 2019).
228. Longhini, L. S., De Almeida Prado, C. P., Bícego, K. C., Zena, L. A. & Gargaglioni, L. H. Measuring cardiorespiratory variables on small tadpoles using a non-invasive methodology. *Rev. Cubana Investig. Biomed.* **38**, (2019).
229. López Rosero, A. C. *Ontogenetic variation of thermal tolerance in two anuran species of Ecuador: Gastrotheca pseustes (Hemiphractidae) and Smilisca phaeota (Hylidae) and their relative vulnerability to environmental temperature change* (Pontificia Universidad Católica Del Ecuador, 2015).
230. Lotshaw, D. P. Temperature adaptation and effects of thermal acclimation in Rana sylvatica and Rana catesbeiana. *Comp. Biochem. Physiol. A Physiol.* **56**, 287–294 (1977).
231. Lu, H.-L., Wu, Q., Geng, J. & Dang, W. Swimming performance and thermal resistance of juvenile and adult newts acclimated to different temperatures. *Acta Herpetol.* **11**, 189–195 (2016).
232. Lu, H. L., Geng, J., Xu, W., Ping, J. & Zhang, Y. P. Physiological response and changes in swimming performance after thermal acclimation in juvenile Chinese fire-belly newts, Cynops orientalis. *Acta Ecol. Sin.* **37**, 1603–1610 (2017).
233. Lutterschmidt, W. I. & Hutchison, V. H. The critical thermal maximum: Data to support the onset of spasms as the definitive end point. *Can. J. Zool.* **75**, 1553–1560 (1997).
234. Madalozzo, B. *Variação latitudinal nos limites de tolerância e plasticidade térmica em anfíbios em um cenário de mudanças climáticas: efeito dos micro-habitats, sazonalidade e filogenia* (Universidade Federal de Santa Maria, 2018).
235. Mahoney, J. J. & Hutchison, V. H. Photoperiod acclimation and 24-hour variations in the critical thermal maxima of a tropical and a temperate frog. *Oecologia* **2**, 143–161 (1969).
236. Maness, J. D. & Hutchison, V. H. Acute adjustment of thermal tolerance in vertebrate ectotherms following exposure to critical thermal maxima. *J. Therm. Biol.* **5**, 225–233 (1980).
237. Manis, M. L. & Claussen, D. L. Environmental and genetic influences on the thermal physiology of Rana sylvatica. *J. Therm. Biol.* **11**, 31–36 (1986).
238. Markle, T. M. & Kozak, K. H. Low acclimation capacity of narrow-ranging thermal specialists exposes susceptibility to global climate change. *Ecol. Evol.* **8**, 4644–4656 (2018).
239. Marshall, E. & Grigg, G. C. Acclimation of CTM, LD50, and rapid loss of acclimation of thermal preferendum in tadpoles of Limnodynastes peronii (Anura, Myobatrachidae). *Aust. Zool.* **20**, 447–456 (1980).

240. Mathias, J. H. *The comparative ecologies of two species of Amphibia (B. bufo and B. calamita) on the Ainsdale Sand Dunes National Nature Reserve* (The University of Manchester, 1971).
241. McManus, J. J. & Nellis, D. W. The critical thermal maximum of the marine toad, Bufo marinus. *Caribb. J. Sci.* **15**, 67–70 (1975).
242. Menke, M. E. & Claussen, D. L. Thermal acclimation and hardening in tadpoles of the bullfrog, Rana catesbeiana. *J. Therm. Biol.* **7**, 215–219 (1982).
243. Merino-Viteri, A. R. *The vulnerability of microhylid frogs, Cophixalus spp., to climate change in the Australian Wet Tropics* (James Cook University, 2018).
244. Messerman, A. F. *Tales of an 'Invisible' Life Stage: Survival and Physiology Among Terrestrial Juvenile Ambystomatid Salamanders* (University of Missouri, 2019).
245. Meza-Parral, Y., García-Robledo, C., Pineda, E., Escobar, F. & Donnelly, M. A. Standardized ethograms and a device for assessing amphibian thermal responses in a warming world. *J. Therm. Biol.* **89**, (2020).
246. Miller, K. & Packard, G. C. Critical thermal maximum: Ecotypic variation between montane and piedmont chorus frogs (Pseudacris triseriata, Hylidae). *Experientia* **30**, 355–356 (1974).
247. Miller, K. & Packard, G. C. An altitudinal cline in critical thermal maxima of chorus frogs (Pseudacris triseriata). *Am. Nat.* **111**, 267–277 (1977).
248. Mueller, C. A., Bucsky, J., Korito, L. & Manzanares, S. Immediate and persistent effects of temperature on oxygen consumption and thermal tolerance in embryos and larvae of the Baja California chorus frog, Pseudacris hypochondriaca. *Front. Physiol.* **10**, (2019).
249. Navas, C. A., Antoniazzi, M. M., Carvalho, J. E., Suzuki, H. & Jared, C. Physiological basis for diurnal activity in dispersing juvenile Bufo granulosus in the Caatinga, a Brazilian semi-arid environment. *Comp. Biochem. Physiol. A Mol. Integr. Physiol.* **147**, 647–657 (2007).
250. Navas, C. A., Úbeda, C. A., Logares, R. & Jara, F. G. Thermal tolerances in tadpoles of three species of Patagonian anurans. *South Am. J. Herpetol.* **5**, 89–96 (2010).
251. Nietfeldt, J. W., Jones, S. M., Droge, D. L. & Ballinger, R. E. Rate of thermal acclimation of larval Ambystoma tigrinum. *J. Herpetol.* **14**, 209–211 (1980).
252. Nol, Rosemarie & Ultsch, G. R. The roles of temperature and dissolved oxygen in microhabitat selection by the tadpoles of a frog (Rana pipiens) and a toad (Bufo terrestris). *Copeia* **1981**, 645–652 (1981).
253. Novarro, A. J. *Thermal physiology in a widespread lungless salamander* (University of Maryland, 2018).
254. Nowakowski, A. J. *et al.* Thermal biology mediates responses of amphibians and reptiles to habitat modification. *Ecol. Lett.* **21**, 345–355 (2018).
255. Nowakowski, A. J. *et al.* Tropical amphibians in shifting thermal landscapes under land-use and climate change. *Conserv. Biol.* **31**, 96–105 (2017).

256. Orille, A. C., McWhinnie, R. B., Brady, S. P. & Raffel, T. R. Positive effects of acclimation temperature on the critical thermal maxima of Ambystoma mexicanum and Xenopus laevis. *J. Herpetol.* **54**, 289–292 (2020).
257. Oyamaguchi, H. M. *et al.* Thermal sensitivity of a Neotropical amphibian (Engystomops pustulosus) and its vulnerability to climate change. *Biotropica* **50**, 326–337 (2018).
258. Paez Vacas, M. I. *Mechanisms of population divergence along elevational gradients in the tropics* (Colorado State University, 2016).
259. Paulson, B. K. & Hutchison, V. H. Blood changes in Bufo cognatus following acute heat stress. *Comp. Biochem. Physiol. A Physiol.* **87**, 461–466 (1987).
260. Paulson, B. & Hutchison, V. Origin of the stimulus for muscular spasms at the critical thermal maximum in anurans. *Copeia* **1987**, 810–813 (1987).
261. Percino-Daniel, R. *et al.* Environmental heterogeneity shapes physiological traits in tropical direct-developing frogs. *Ecol. Evol.* (2021).
262. Perotti, M. G., Bonino, M. F., Ferraro, D. & Cruz, F. B. How sensitive are temperate tadpoles to climate change? The use of thermal physiology and niche model tools to assess vulnerability. *Zoology* **127**, 95–105 (2018).
263. Pintanel, P., Tejedo, M., Almeida-Reinoso, F., Merino-Viteri, A. & Gutiérrez-Pesquera, L. M. Critical thermal limits do not vary between wild-caught and captive-bred tadpoles of Agalychnis spurrelli (Anura: Hylidae). *Diversity* **12**, (2020).
264. Pintanel, P., Tejedo, M., Ron, S. R., Llorente, G. A. & Merino-Viteri, A. Elevational and microclimatic drivers of thermal tolerance in Andean Pristimantis frogs. *J. Biogeogr.* **46**, 1664–1675 (2019).
265. Pintanel, P. *Thermal adaptation of amphibians in tropical mountains. Consequences of global warming* (Universitat de Barcelona, 2018).
266. Pintanel, P., Tejedo, M., Salinas-Ivanenko, S., Jervis, P. & Merino-Viteri, A. Predators like it hot: Thermal mismatch in a predator-prey system across an elevational tropical gradient. *J. Anim. Ecol.* (2021).
267. Pough, F. H. Natural daily temperature acclimation of eastern red efts, Notophthalmus v. viridescens (Rafinesque) (Amphibia: Caudata). *Comp. Biochem. Physiol. A Physiol.* **47**, 71–78 (1974).
268. Pough, F. H., Stewart, M. M. & Thomas, R. G. Physiological basis of habitat partitioning in Jamaican Eleutherodactylus. *Oecologia* **27**, 285–293 (1977).
269. Quiroga, L. B., Sanabria, E. A., Fornés, M. W., Bustos, D. A. & Tejedo, M. Do sublethal concentrations of chlorpyrifos induce changes in the thermal sensitivity and tolerance of anuran tadpoles in the toad Rhinella arenarum? *Chemosphere* **219**, 671–677 (2019).
270. Rausch, C. *The thermal ecology of the Red-spotted toad, Bufo punctatus, across life history* (University of Nevada, 2007).

271. Reichenbach, N. & Brophy, T. R. Natural history of the Peaks of Otter salamander (Plethodon hubrichti) along an elevational gradient. *Herpetol. Bull.* 7–15 (2017).
272. Reider, K. E., Larson, D. J., Barnes, B. M. & Donnelly, M. A. Thermal adaptations to extreme freeze–thaw cycles in the high tropical Andes. *Biotropica* **53**, 296–306 (2021).
273. Richter-Boix, A. *et al.* Local divergence of thermal reaction norms among amphibian populations is affected by pond temperature variation. *Evolution* **69**, 2210–2226 (2015).
274. Riquelme, N. A., Díaz-Páez, H. & Ortiz, J. C. Thermal tolerance in the Andean toad Rhinella spinulosa (Anura: Bufonidae) at three sites located along a latitudinal gradient in Chile. *J. Therm. Biol.* **60**, 237–245 (2016).
275. Ritchart, J. P. & Hutchison, V. H. The effects of ATP and cAMP on the thermal tolerance of the mudpuppy, Necturus maculosus. *J. Therm. Biol.* **11**, 47–51 (1986).
276. Rivera-Burgos, A. C. *Habitat suitability for Eleutherodactylus frogs in Puerto Rico: Indexing occupancy, abundance and reproduction to climatic and habitat characteristics* (North Carolina State University, 2019).
277. Rivera-Ordonez, J. M., Nowakowski, A. J., Manansala, A., Thompson, M. E. & Todd, B. D. Thermal niche variation among individuals of the poison frog, Oophaga pumilio, in forest and converted habitats. *Biotropica* **51**, 747–756 (2019).
278. Romero Barreto, P. *Requerimientos fisiológicos y microambientales de dos especies de anfibios (Scinax ruber e Hyloxalus yasuni) del bosque tropical de Yasuní y sus implicaciones ante el cambio climático* (Pontificia Universidad Católica Del Ecuador, 2013).
279. Ruiz-Aravena, M. *et al.* Impact of global warming at the range margins: Phenotypic plasticity and behavioral thermoregulation will buffer an endemic amphibian. *Ecol. Evol.* **4**, 4467–4475 (2014).
280. Ruthsatz, K. *et al.* Thyroid hormone levels and temperature during development alter thermal tolerance and energetics of Xenopus laevis larvae. *Conserv. Physiol.* **6**, (2018).
281. Ruthsatz, K. *et al.* Post-metamorphic carry-over effects of altered thyroid hormone level and developmental temperature: physiological plasticity and body condition at two life stages in Rana temporaria. *J. Comp. Physiol. B* **190**, 297–315 (2020).
282. Rutledge, P. S., Spotila, J. R. & Easton, D. P. Heat hardening in response to two types of heat shock in the lungless salamanders Eurycea bislineata and Desmognathus ochrophaeus. *J. Therm. Biol.* **12**, 235–241 (1987).
283. Sanabria, E. *et al.* Effect of salinity on locomotor performance and thermal extremes of metamorphic Andean Toads (Rhinella spinulosa) from Monte Desert, Argentina. *J. Therm. Biol.* **74**, 195–200 (2018).
284. Sanabria, E. A., González, E., Quiroga, L. B. & Tejedo, M. Vulnerability to warming in a desert amphibian tadpole community: the role of interpopulational variation. *J. Zool.* **313**, 283–296 (2021).

285. Sanabria, E. A. & Quiroga, L. B. Change in the thermal biology of tadpoles of Odontophrynus occidentalis from the Monte desert, Argentina: Responses to photoperiod. *J. Therm. Biol.* **36**, 288–291 (2011).
286. Sanabria, E. A., Quiroga, L. B., González, E., Moreno, D. & Cataldo, A. Thermal parameters and locomotor performance in juvenile of Pleurodema nebulosum (Anura: Leptodactylidae) from the Monte Desert. *J. Therm. Biol.* **38**, 390–395 (2013).
287. Sanabria, E. A., Quiroga, L. B. & Martino, A. L. Seasonal changes in the thermal tolerances of the toad Rhinella arenarum (Bufonidae) in the Monte Desert of Argentina. *J. Therm. Biol.* **37**, 409–412 (2012).
288. Sanabria, E. A., Quiroga, L. B. & Martino, A. L. Seasonal changes in the thermal tolerances of Odontophrynus occidentalis (Berg, 1896) (Anura: Cycloramphidae). *Belg. J. Zool.* **143**, 23–29 (2013).
289. Sanabria, E. A. *et al.* Thermal ecology of the post-metamorphic Andean toad (Rhinella spinulosa) at elevation in the Monte Desert, Argentina. *J. Therm. Biol.* **52**, 52–57 (2015).
290. Sanabria, E. A., Vaira, M., Quiroga, L. B., Akmentins, M. S. & Pereyra, L. C. Variation of thermal parameters in two different color morphs of a diurnal poison toad, Melanophryniscus rubriventris (Anura: Bufonidae). *J. Therm. Biol.* **41**, 1–5 (2014).
291. Sanabria, E. A. & Quiroga, L. B. Thermal parameters changes in males of Rhinella arenarum (Anura: Bufonidae) related to reproductive periods. *Rev. Biol. Trop.* **59**, 347–353 (2011).
292. Scheffers, B. R. *et al.* Thermal buffering of microhabitats is a critical factor mediating warming vulnerability of frogs in the Philippine biodiversity hotspot. *Biotropica* **45**, 628–635 (2013).
293. Scheffers, B. R., Edwards, D. P., Diesmos, A., Williams, S. E. & Evans, T. A. Microhabitats reduce animals' exposure to climate extremes. *Glob. Change Biol.* **20**, 495–503 (2014).
294. Schmid, W. D. High temperature tolerances of Bufo hemiophrys and Bufo cognatus. *Ecology* **46**, 559–560 (1965).
295. Sealer, J. A. & West, B. W. Critical thermal maxima of some Arkansas salamanders in relation to thermal acclimation. *Herpetologica* **25**, 122–124 (1969).
296. Seibel, R. V. Variables affecting the critical thermal maximum of the leopard frog, Rana pipiens Schreber. *Herpetologica* **26**, 208–213 (1970).
297. Sherman, E. Ontogenetic change in thermal tolerance of the toad Bufo woodhousii fowleri. *Comp. Biochem. Physiol. A Physiol.* **65**, 227–230 (1980).
298. Sherman, E. Thermal biology of newts (Notophthalmus viridescens) chronically infected with a naturally occurring pathogen. *J. Therm. Biol.* **33**, 27–31 (2008).
299. Sherman, E., Baldwin, L., Fernández, G. & Deurell, E. Fever and thermal tolerance in the toad Bufo marinus. *J. Therm. Biol.* **16**, 297–301 (1991).
300. Sherman, E. & Levitis, D. Heat hardening as a function of developmental stage in larval and juvenile Bufo americanus and Xenopus laevis. *J. Therm. Biol.* **28**, 373–380 (2003).

301. Shi, L., Zhao, L., Ma, X. & Ma, X. Selected body temperature and thermal tolerance of tadpoles of two frog species (Fejervarya limnocharis and Microhyla ornata) acclimated under different thermal conditions. *Acta Ecol. Sin.* **32**, 0465–0471 (2012).
302. Simon, M. N., Ribeiro, P. L. & Navas, C. A. Upper thermal tolerance plasticity in tropical amphibian species from contrasting habitats: Implications for warming impact prediction. *J. Therm. Biol.* **48**, 36–44 (2015).
303. Simon, M. *Plasticidade fenotípica em relação à temperatura de larvas de Rhinella (Anura: Bufonidae) da caatinga e da floresta Atlântica* (Universidade de Sao Paulo, 2010).
304. Skelly, D. K. & Freidenburg, L. K. Effects of beaver on the thermal biology of an amphibian. *Ecol. Lett.* **3**, 483–486 (2000).
305. Sos, T. Thermoconformity even in hot small temporary water bodies: a case study in yellow-bellied toad (Bombina v. variegata). *Herpetologica Romanica* **1**, 1–11 (2007).
306. Spotila, J. R. Role of temperature and water in the ecology of lungless salamanders. *Ecol. Monogr.* **42**, 95–125 (1972).
307. Tracy, C. R., Christian, K. A., Betts, G. & Tracy, C. R. Body temperature and resistance to evaporative water loss in tropical Australian frogs. *Comp. Biochem. Physiol. A Mol. Integr. Physiol.* **150**, 102–108 (2008).
308. Turriago, J. L., Parra, C. A. & Bernal, M. H. Upper thermal tolerance in anuran embryos and tadpoles at constant and variable peak temperatures. *Can. J. Zool.* **93**, 267–272 (2015).
309. Vidal, M. A., Novoa-Muñoz, F., Werner, E., Torres, C. & Nova, R. Modeling warming predicts a physiological threshold for the extinction of the living fossil frog Calyptocephalella gayi. *J. Therm. Biol.* **69**, 110–117 (2017).
310. von May, R. *et al.* Divergence of thermal physiological traits in terrestrial breeding frogs along a tropical elevational gradient. *Ecol. Evol.* **7**, 3257–3267 (2017).
311. von May, R. *et al.* Thermal physiological traits in tropical lowland amphibians: Vulnerability to climate warming and cooling. *PLoS ONE* **14**, (2019).
312. Wagener, C., Kruger, N. & Measey, J. Progeny of Xenopus laevis from altitudinal extremes display adaptive physiological performance. *J. Exp. Biol.* **224**, (2021).
313. Wang, H. & Wang, L. Thermal adaptation of the common giant toad (Bufo gargarizans) at different earlier developmental stages. *J. Agric. Univ. Hebei* **31**, 79–83 (2008).
314. Wang, L. The effects of constant and variable thermal acclimation on thermal tolerance of the common giant toad tadpoles (Bufo gargarizans). *Acta Ecol. Sin.* **34**, 1030–1034 (2014).
315. Wang, L.-Z. & Li, X.-C. Effect of temperature on incubation and thermal tolerance of the Chinese forest frog. *Chin. J. Zool.* (2007).
316. Wang, L. & Li, X.-C. Effects of constant thermal acclimation on thermal tolerance of the Chinese forest frog (Rana chensinensis). *Acta Hydrobiol. Sin.* **31**, 748–750 (2007).

317. Wang, L.-Z., Li, X.-C. & Sun, T. Preferred temperature, avoidance temperature and lethal temperature of tadpoles of the common giant toad (Bufo gargarizans) and the Chinese forest frog (Rana chensinensis). *Chin. J. Zool.* **40**, 23–27 (2005).
318. Warburg, M. R. On the water economy of Israel amphibians: The anurans. *Comp. Biochem. Physiol. A Physiol.* **40**, 911–924 (1971).
319. Warburg, M. R. The water economy of Israel amphibians: The urodeles Triturus vittatus (Jenyns) and Salamandra salamandra (L.). *Comp. Biochem. Physiol. A Physiol.* **40**, 1055–1063 (1971).
320. Willhite, C. & Cupp, P. V. Daily rhythms of thermal tolerance in Rana clamitans (Anura: Ranidae) tadpoles. *Comp. Biochem. Physiol. A Physiol.* **72**, 255–257 (1982).
321. Wu, C.-S. & Kam, Y.-C. Thermal tolerance and thermoregulation by Taiwanese rhacophorid tadpoles (Buergeria japonica) living in geothermal hot springs and streams. *Herpetologica* **61**, 35–46 (2005).
322. Wu, Q.-H. & Hsieh, C.-H. Thermal tolerance and population genetics of Hynobius fuca. (No abbreviation found; *Thermal tolerance...*) *64*, (2016).
323. Xu, X. *The effect of temperature on body temperature and thermoregulation in different geographic populations of Rana dybowskii* (Harbin Normal University, 2017).
324. Yandún Vela, M. C. *Capacidad de aclimatación en renacuajos de dos especies de anuros: Rhinella marina (Bufonidae) y Gastrotheca riobambae (Hemiphractidae) y su vulnerabilidad al cambio climático* (Pontificia Universidad Católica Del Ecuador, 2017).
325. Young, V. K. H. & Gifford, M. E. Limited capacity for acclimation of thermal physiology in a salamander, Desmognathus brimleyorum. *J. Comp. Physiol. B* **183**, 409–418 (2013).
326. Yu, Z., Dickstein, R., Magee, W. E. & Spotila, J. R. Heat shock response in the salamanders Plethodon jordani and Plethodon cinereus. *J. Therm. Biol.* **23**, 259–265 (1998).
327. Zheng, R.-Q. & Liu, C.-T. Giant spiny-frog (Paa spinosa) from different populations differ in thermal preference but not in thermal tolerance. *Aquat. Ecol.* **44**, 723–729 (2010).
328. Zweifel, R. G. Studies on the critical thermal maxima of salamanders. *Ecology* **38**, 64–69 (1957).

Acknowledgements

This study was funded by UNSW Scientia Doctoral Scholarships awarded to PPottier, SB, and PPollo. SN was supported by the Australian Research Council (ARC) Discovery Project (DP210100812). SMD was supported by the ARC Discovery Early Career Award (DE180100202). MRK was supported by the ARC Discovery Project DP200101279. We thank the authors of the original studies who provided the groundwork for our analyses. We pay our respects to the Bedegal people, the traditional custodians of the land on which this work was primarily conducted.

Authors' contributions

This study was conceptualized by PPottier, MRK, SB, SMD, and SN. All data manipulation and analyses were performed by PPottier (with conceptual and technical input from SMD and SN for the imputation methods and statistical analyses, MRK, ARG, JER, and NCW for the biophysical modelling and climate vulnerability analyses). All code was reviewed by NCW, ARG, and JER following the recommendations of [115]. Ecotype information was collected by NCW, PPollo, and ANRV. PPottier, NCW, and SMD contributed to data visualization. PPottier wrote the initial draft, and all authors were involved in the review and editing. PPottier oversaw the project administration, while SMD and SN were in charge of the supervision.

Inclusion & ethics statement

This study did not involve researchers who collected the original data. All data used for the analyses were taken from a previous data compilation[3], and original references on which all analyses were built upon are listed in the Methods references[116-328].

Competing interest declaration

The authors declare no conflict or competing interests.

Additional information

Supplementary Information is available for this paper. Correspondence and requests for materials should be addressed to Patrice Pottier. Reprints and permissions information is available at www.nature.com/reprints.

Extended data figures

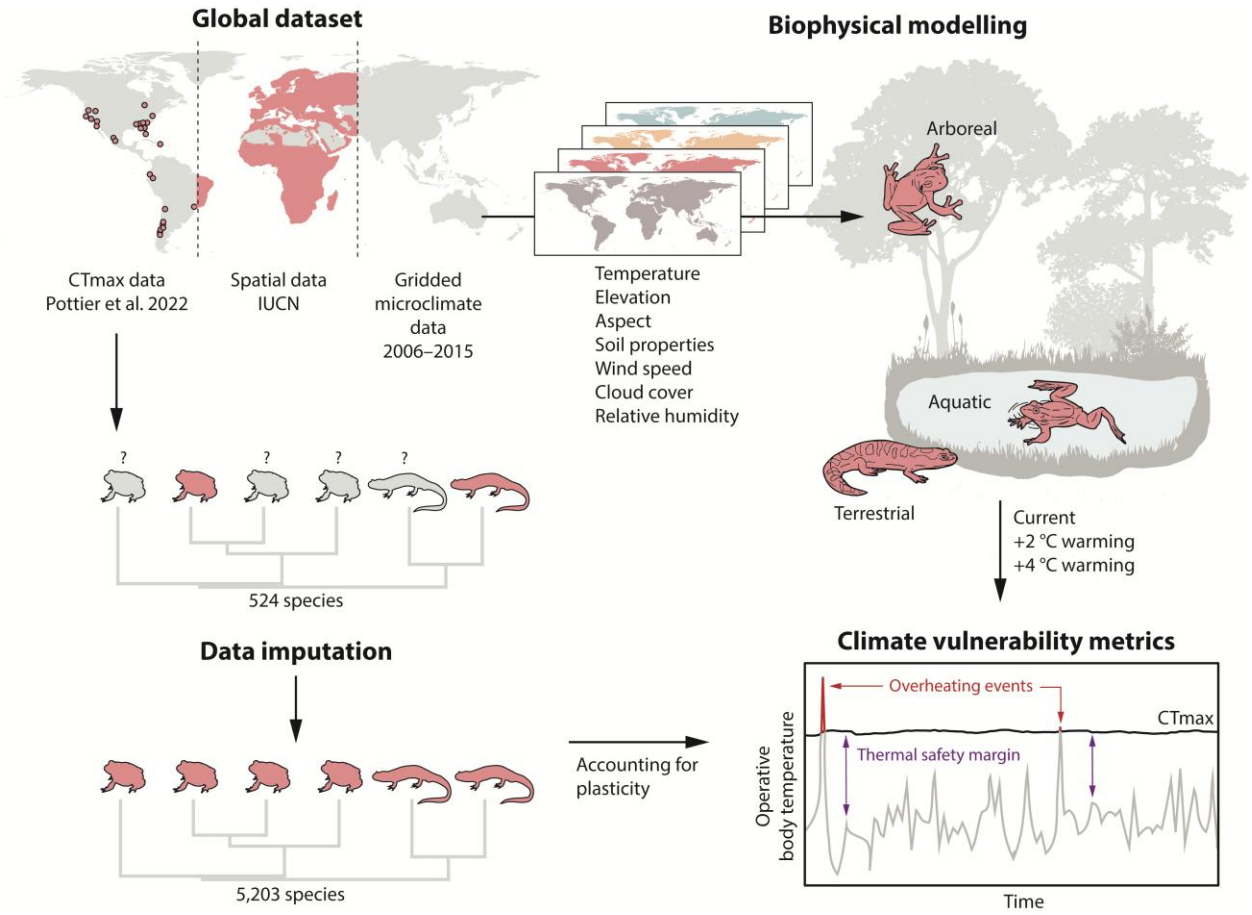

Extended Data Fig. 1 | Conceptual overview of the methods employed to assess the vulnerability of amphibians to global warming.

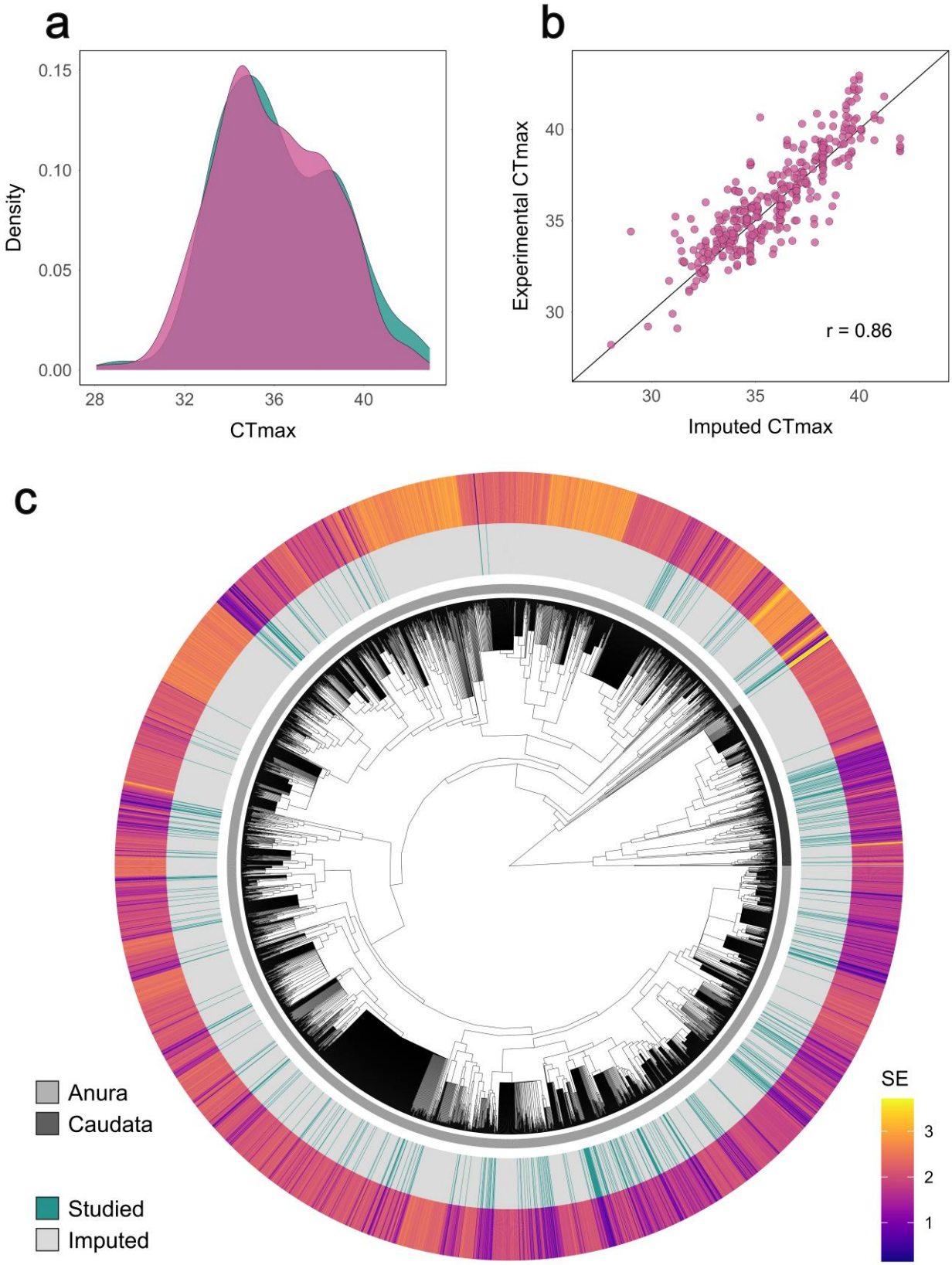

Extended Data Fig. 2 | Accuracy of the data imputation procedure. a) Probability density distributions (n = 375 observations, 77 species) of experimental CT_{max} (blue) and CT_{max} cross-validated using our data imputation procedure (pink). b) Correlation between experimental and imputed CT_{max} values. c) Variation in the uncertainty (standard error, SE) of imputed CT_{max} predictions (outer heat map) across studied (blue; n = 524) and imputed (grey; n = 4,679) species.

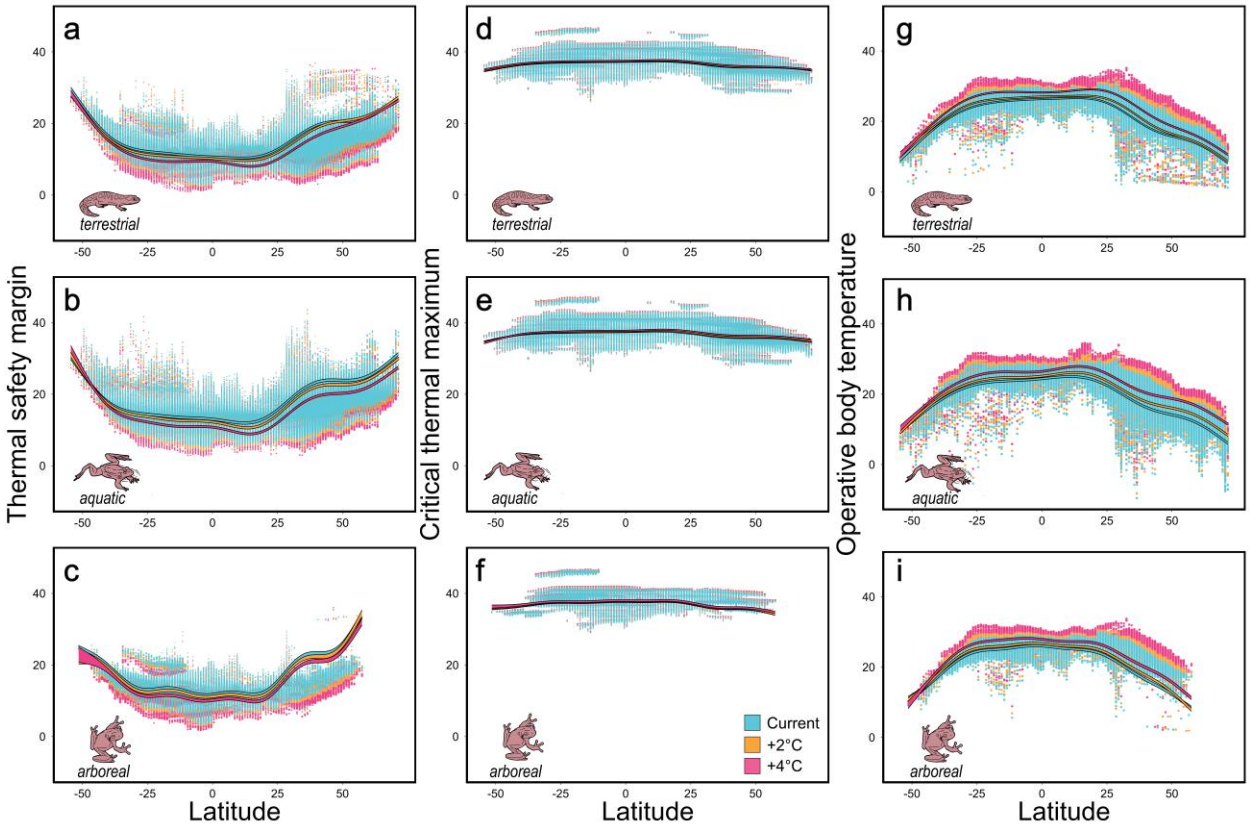

Extended Data Fig. 3 | Thermal safety margin, critical thermal maximum, and operative body temperatures in different microhabitats and climatic scenarios. Weighted mean thermal safety margins (TSM; a-c), critical thermal maximum (CT_{max}; d-f) and operative body temperatures (g-i) in terrestrial (a,d,g), aquatic (b,e,h) and arboreal (c,f,i) microhabitats are depicted in current microclimates (blue data points), or assuming 2°C and 4°C of global warming above pre-industrial levels (orange, and pink data points, respectively) across latitudes, for each local species occurrence (n = 203,853 for terrestrial species; n = 204,808 for aquatic species; n = 56,210 for aquatic species). Lines represent 95% confidence intervals of model predictions from generalised additive mixed models. CT_{max} and TSM estimates are scaled by precision (1/s.e.), with smaller points indicating higher uncertainty. Each point represents a species in a given grid cell.

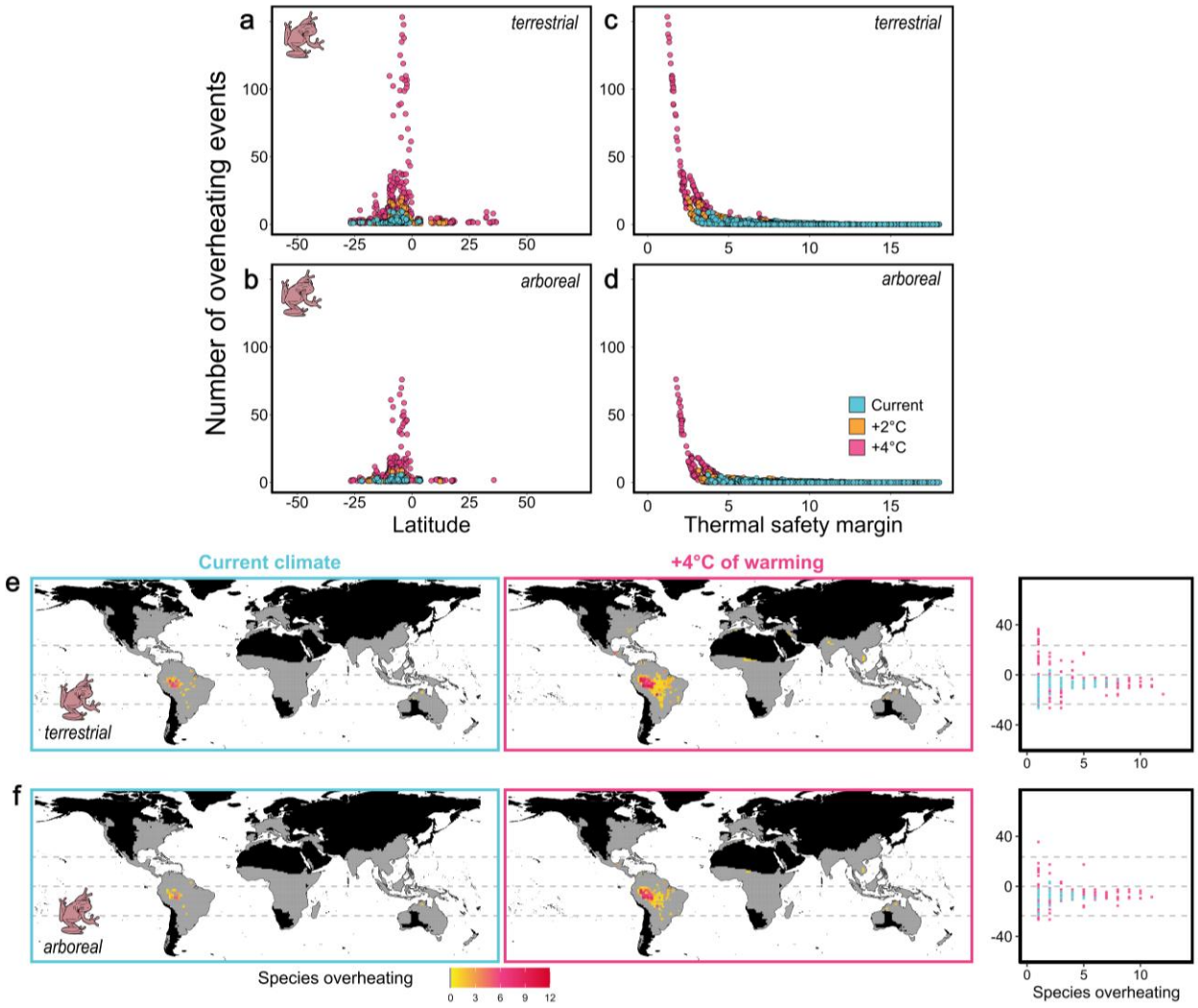

Extended Data Fig. 4 | Vulnerability of arboreal amphibians in terrestrial and arboreal microhabitats. Depicted are the number of overheating events experienced by arboreal species across latitudes (a-b) and in relation to thermal safety margins (c-d) in terrestrial (a-c) and arboreal microhabitats (b-d). The number of overheating events were calculated based on the mean probability that daily maximum temperatures exceeded CT_{max} during the warmest quarters of 2006-2015 for each species in each grid cell (i.e., local species occurrence; n = 203,853 for terrestrial species; n = 204,808 for aquatic species; n = 56,210 for aquatic species). Blue points depict the number of overheating events in historical microclimates, while orange and pink points depict the number of overheating events assuming 2°C and 4°C of global warming above pre-industrial levels, respectively. In panel a) and b), only the species predicted to overheat for at least one day are displayed. The number of arboreal species predicted to experience overheating events in terrestrial (e) and arboreal (f) microhabitats in each assemblage is also depicted. The number of species overheating was assessed as the sum of species overheating for at least one day in the period surveyed (warmest quarters of 2006-2015) in each assemblage (1-degree grid cell; n = 14,090 for terrestrial species; n = 14,091 for aquatic species; n = 6,614 for arboreal species). Black colour depicts areas with no data, and grey colour assemblages without species at risk. The right panel depicts latitudinal patterns in the number of species predicted to overheat in current climates (blue) or assuming 4°C of global warming above pre-industrial levels (pink). Dashed lines represent the equator and tropics. Few species (n = 11) were predicted to experience overheating events in water bodies, and hence are not displayed.

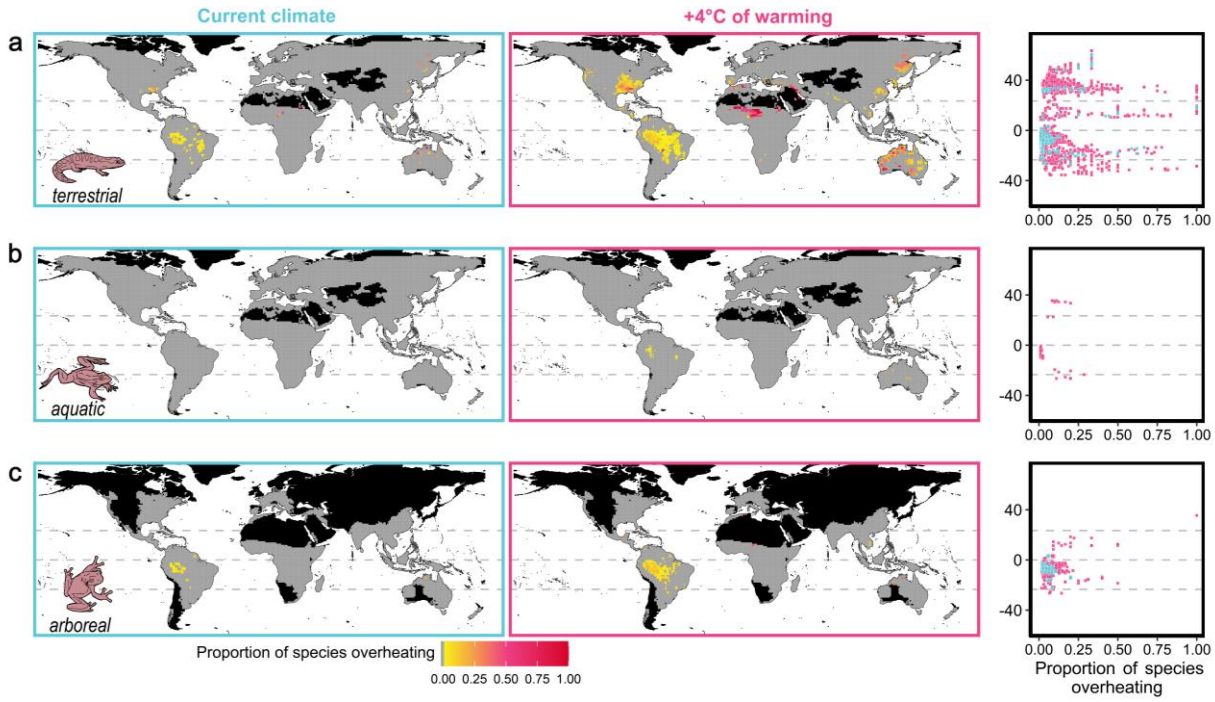

Extended Data Fig. 5 | Proportion of species predicted to experience overheating events in terrestrial (a), aquatic (b), and arboreal (c) microhabitats. The proportion of species overheating was assessed as the sum of species overheating for at least one day in the period surveyed (warmest quarters of 2006-2015) divided by the number of species in each assemblage (1-degree grid cell; n = 14,090 for terrestrial species; n = 14,091 for aquatic species; n = 6,614 for arboreal species). Black colour depicts areas with no data, and grey colour assemblages without species at risk. The right panel depicts latitudinal patterns in the proportion of species predicted to overheat in current climates (blue) or assuming 4°C of global warming above pre-industrial levels (pink). Dashed lines represent the equator and tropics.

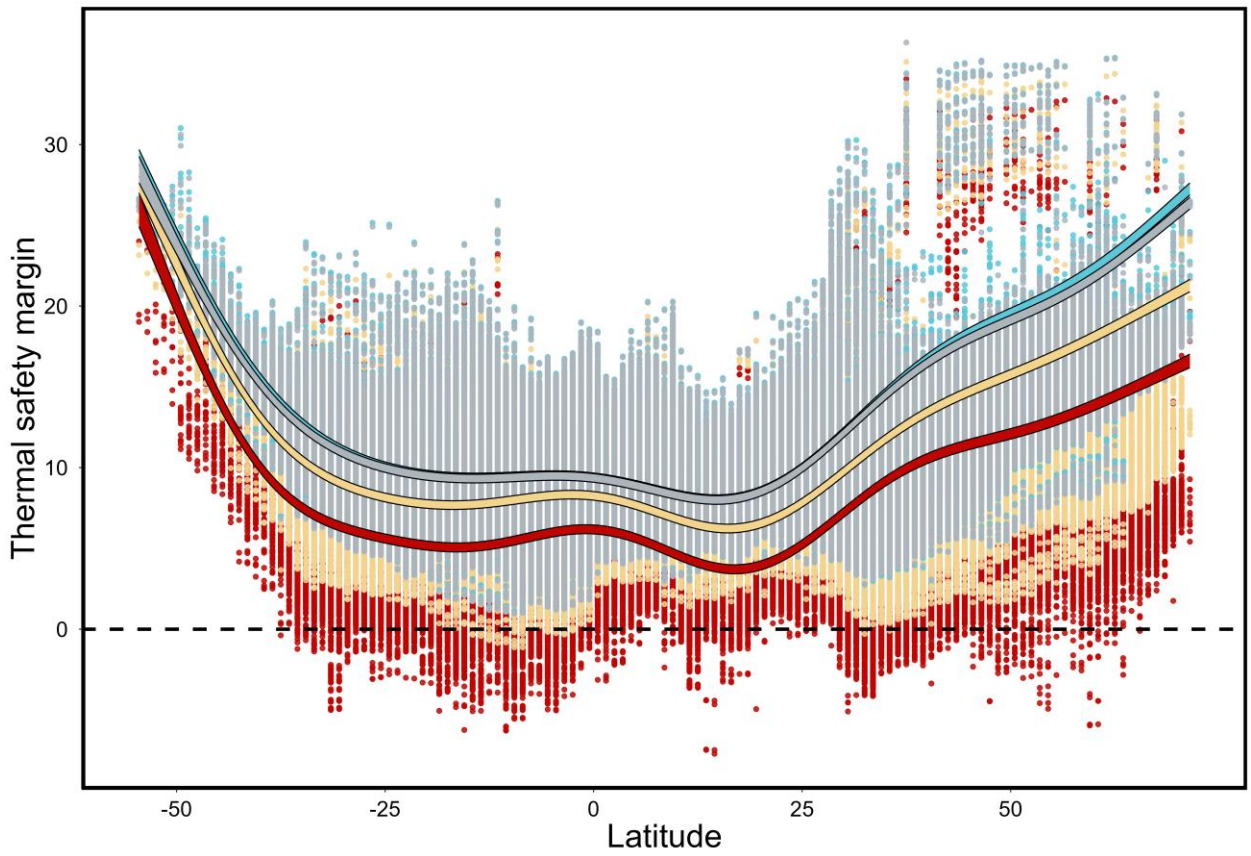

Extended Data Fig. 6 | Variation in thermal safety margins calculated using different assumptions. Thermal safety margins (TSM) were calculated as the mean difference between CT_{max} and the predicted operative body temperature in full shade during the warmest quarters of 2006-2015 (grey), as the mean difference between CT_{max} and the predicted operative body temperature in full shade during the warmest quarters of 2006-2015 excluding body temperatures falling outside the 5% and 95% percentile temperatures (blue), as the difference between the 95% percentile operative body temperature and the corresponding CT_{max} (yellow), or as the difference between the maximum operative body temperature and the corresponding CT_{max} (red). Lines represented 95% confidence interval ranges predicted from generalized additive mixed models. This figure was constructed assuming ground-level microclimates occurring under 4°C of global warming above pre-industrial levels, for each species in each grid cell (i.e., local species occurrences; n = 203,853 for terrestrial species; n = 204,808 for aquatic species; n = 56,210 for aquatic species).

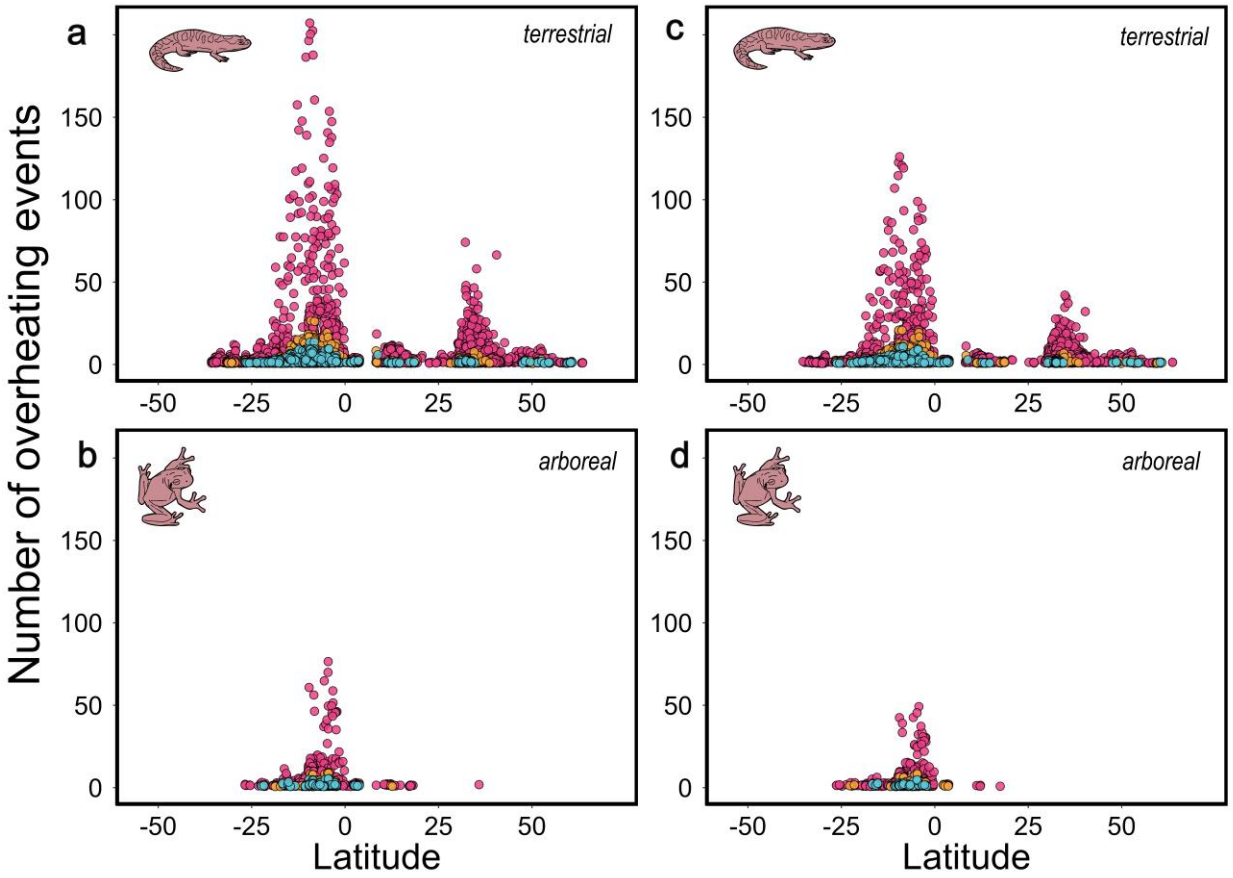

Extended Data Fig. 7 | Latitudinal variation in the number of overheating events when animals are acclimated to the mean (a,b) or maximum (c,d) weekly body temperature experienced in the seven days prior in terrestrial (a,c) and arboreal (b,d) microhabitats. The number of overheating events (days) were calculated based on the mean probability that daily maximum temperatures exceeded CT_{max} during the warmest quarters of 2006-2015 for each species in each grid cell (i.e., local species occurrences; n = 203,853 for terrestrial species; n = 204,808 for aquatic species; n = 56,210 for aquatic species). Blue points depict the number of overheating events in historical microclimates, while orange and pink points depict the number of overheating events assuming 2°C and 4°C of global warming above pre-industrial levels, respectively. For clarity, only the species predicted to experience overheating events across latitudes are depicted.

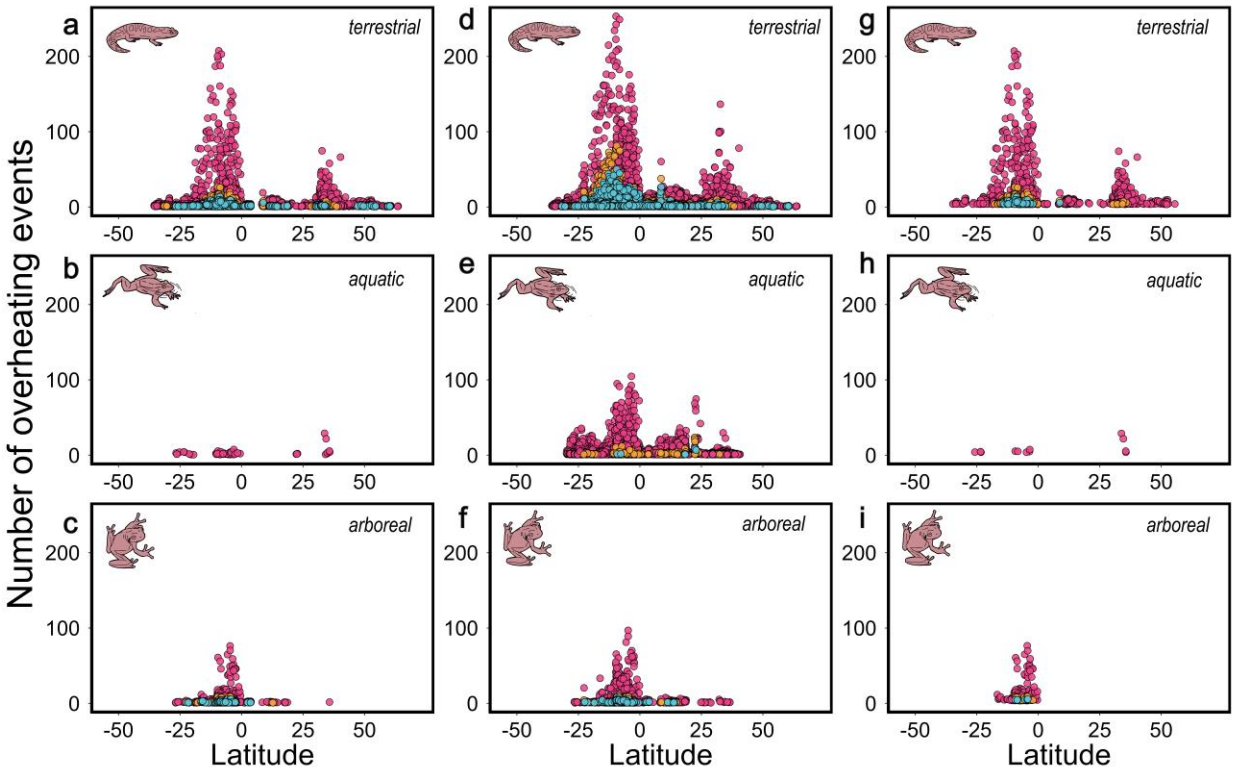

Extended Data Fig. 8 | Latitudinal variation in the number of overheating events using regular (a,b,c), uncertain (d,e,f), or conservative estimates (g,h,i) in terrestrial (a,d,g), aquatic (b,e,h) and arboreal (c,f,i) microhabitats. The number of overheating events (days) were calculated based on the mean probability that daily maximum temperatures exceeded CT_{max} during the warmest quarters of 2006-2015 for each species in each grid cell (i.e., local species occurrences; n = 203,853 for terrestrial species; n = 204,808 for aquatic species; n = 56,210 for aquatic species). Uncertain estimates are those where daily overheating probabilities were calculated based on broad predicted distributions of CT_{max} (i.e., simulated over the whole "*biological range*"), likely inflating overheating probabilities for observations with large uncertainty. Conservative estimates are those when overheating risk was considered only when the 95% confidence intervals of the predicted number of overheating events did not overlap with zero (e,f). Blue points depict the number of overheating events in historical microclimates, while orange and pink points depict the number of overheating events assuming 2°C and 4°C of global warming above pre-industrial levels, respectively. For clarity, only the species predicted to experience overheating events across latitudes are depicted.

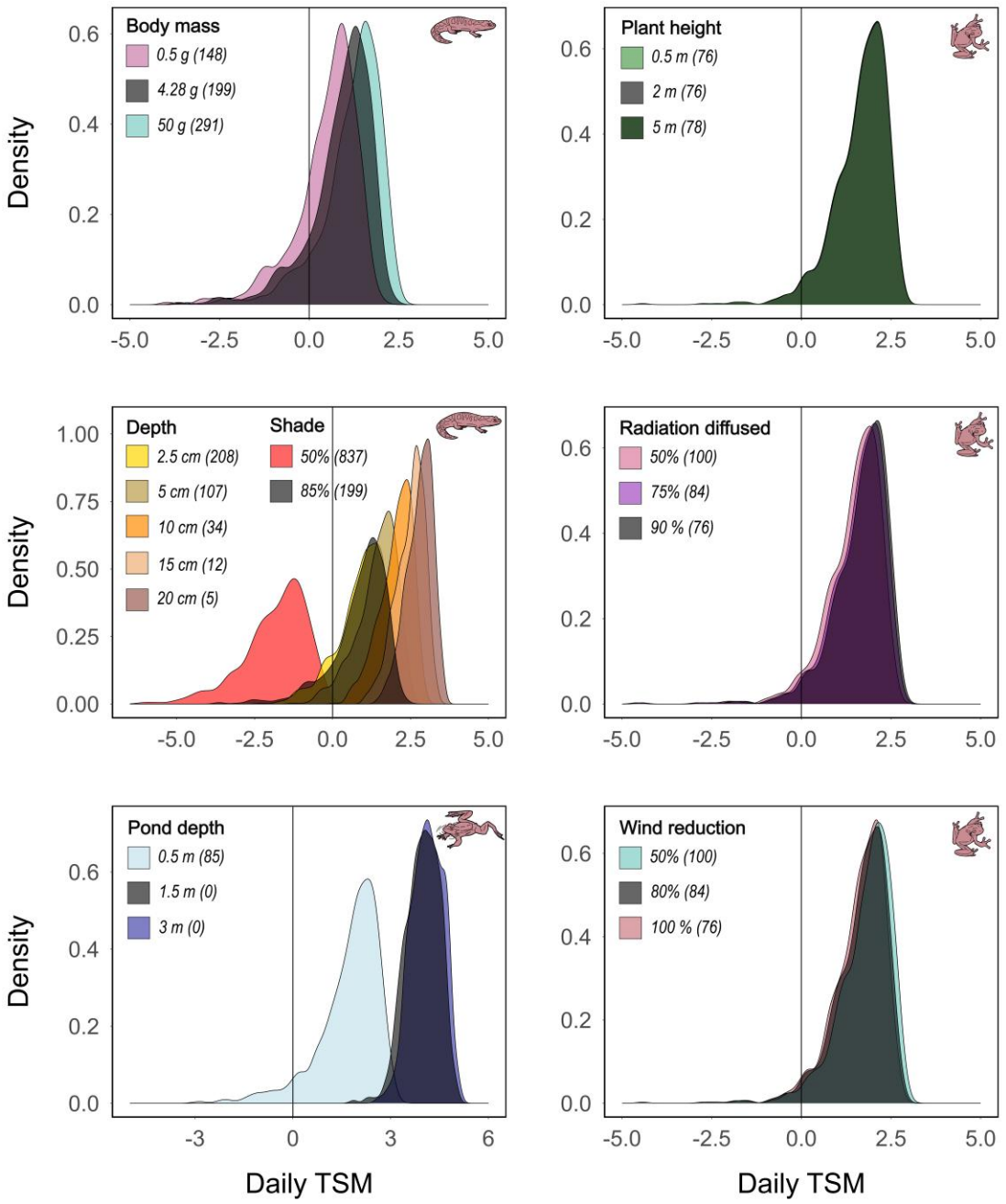

Extended Data Fig. 9 | Influence of biophysical model parameters on the estimation of terrestrial (a,b), aquatic (c), and arboreal (d,e,f) thermal safety margins. Depicted is the variation in daily thermal safety margins (TSM) as density distributions according to body mass (a), shade availability and soil depth (b), pond depth (c), height of the animal in above-ground vegetation (d), percentage of solar radiation diffused by vegetation (e), and percentage of wind reduced by vegetation (f). All simulations were performed assuming 4°C of global warming above pre-industrial levels in a specific grid cell (latitude, longitude = -9.5, -69.5; where the highest number of overheating events was predicted), for the most vulnerable species (*Noblella myrmecoides* in terrestrial and aquatic microhabitats, *Pristimantis ockendeni* in arboreal microhabitats). Negative daily TSMs were recorded as overheating events, and conditions depicted in dark grey reflect the results presented in the manuscript. The number of predicted overheating events is indicated in brackets for each condition (n = 910 days).

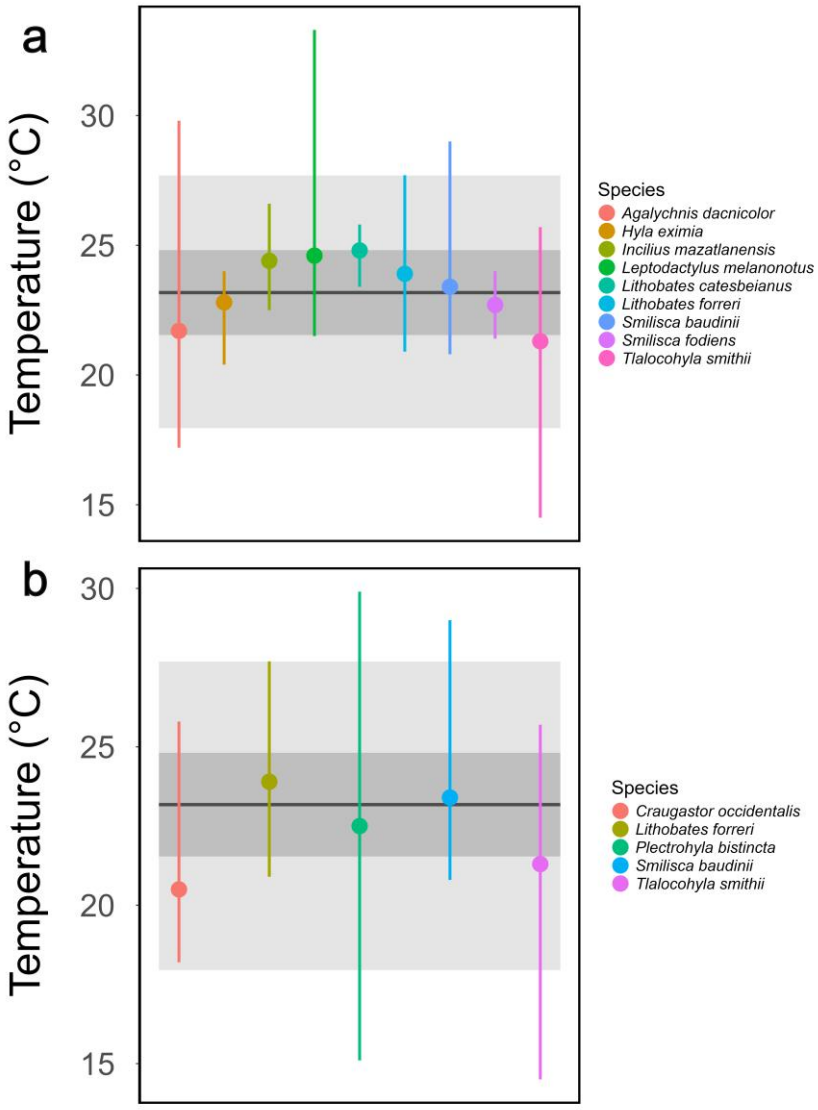

Extended Data Fig. 10 | Validation of operative body temperature estimations. Terrestrial operative body temperatures estimated from biophysical models were compared to field body temperatures recorded around Tepic (21.48° N, -104.85° W; n = 11 species; panel a) and El Cuarenteño (21.45° N, -105.03° W; n = 5 species; panel b) between June and October of 2013/2015, for 11 species of frogs[111]. The mean hourly operative body temperatures predicted from our models for the same date and time windows (18:00 – 01:00) are represented by the black horizontal line, along with their standard deviation (dark grey box), and range (light grey box). The mean (point) and range (bars) of field body temperatures recorded for each species are presented in colour. Note that our analyses were based on the maximum daily temperature recorded at each site during the warmest quarters of 2006-2015, which may not match the times and dates at which field body temperatures were recorded. Nevertheless, congruence between night-time predicted and field body temperatures suggests our models are likely to capture true biological variation in operative body temperatures throughout the day.

Vulnerability of amphibians to global warming

Patrice Pottier[1,2*], Michael R. Kearney[3], Nicholas C. Wu[4], Alex R. Gunderson[5], Julie E. Rej[5], A. Nayelli Rivera-Villanueva[6,7], Pietro Pollo[1], Samantha Burke[1], Szymon M. Drobniak[1,8+], and Shinichi Nakagawa[1,9+]

[1] Evolution & Ecology Research Centre, School of Biological, Earth and Environmental Sciences, University of New South Wales, Sydney, New South Wales, Australia.

[2] Division of Ecology and Evolution, Research School of Biology, The Australian National University, Canberra, Australian Capital Territory, Australia

[3] School of BioSciences, The University of Melbourne, Melbourne, Victoria, Australia

[4] Hawkesbury Institute for the Environment, Western Sydney University, Richmond, New South Wales, Australia

[5] Department of Ecology and Evolutionary Biology, Tulane University, New Orleans, Louisiana, USA

[6] Centro Interdisciplinario de Investigación para el Desarrollo Integral Regional Unidad Durango (CIIDIR), Instituto Politécnico Nacional, Durango, México

[7] Laboratorio de Biología de la Conservación y Desarrollo Sostenible de la Facultad de Ciencias Biológicas, Universidad Autónoma de Nuevo León, Monterrey, México

[8] Institute of Environmental Sciences, Jagiellonian University, Kraków, Poland.

[9] Department of Biological Sciences, University of Alberta, Edmonton, Alberta, Canada.

[*]Corresponding author

[+]These authors supervised the work equally

Corresponding author: Patrice Pottier (p.pottier@unsw.edu.au)

Table of contents

Supplementary tables

Table S1 | Statistical model estimates for thermal safety margins calculated for local species occurrences and assemblages Model estimates for each microhabitat (terrestrial, arboreal, aquatic) and each climatic scenario (current, +2°C, or +4°C of global warming above pre-industrial levels) are depicted. No contrast structure was used in the presented models. mean: mean model estimate; CI.lb: lower bound of the 95% confidence interval; CI.ub: upper bound of the 95% confidence interval; p: p-value; k_{sp}: number of species; k_{obs}: number of observations; Var_{sp}: variance explained by differences between species; Var_{phy}: variance explained by shared evolutionary history; Var_{obs}: residual variance.

	Local species patterns in thermal safety margin								
	mean	**CI.lb**	**CI.ub**	**p**	**k_{sp}**	**k_{obs}**	**Var_{sp}**	**Var_{phy}**	**Var_{obs}**
Terrestrial (current)	11.694	8.856	14.428	<0.001	5177	203853			
Terrestrial (+2°C)	10.914	8.025	13.594	<0.001	5177	203853			
Terrestrial (+4°C)	9.409	6.530	12.090	<0.001	5177	203853			
Arboreal (current)	12.235	9.402	14.960	<0.001	1771	56210			
Arboreal (+2°C)	11.517	8.660	14.236	<0.001	1771	56210	1.295	11.960	1.828
Arboreal (+4°C)	10.073	7.229	12.797	<0.001	1771	56210			
Aquatic (current)	13.598	10.708	16.276	<0.001	5203	204808			
Aquatic (+2°C)	12.827	8.796	14.361	<0.001	5203	204808			
Aquatic (+4°C)	11.682	8.796	14.361	<0.001	5203	204808			

	Assemblage-level patterns in thermal safety margin					
	mean	**CI.lb**	**CI.ub**	**p**	**k_{obs}**	**Var_{obs}**
Terrestrial (current)	15.279	15.208	15.330	<0.001	14090	
Terrestrial (+2°C)	14.328	14.279	14.396	<0.001	14090	
Terrestrial (+4°C)	12.602	12.542	12.657	<0.001	14090	
Arboreal (current)	14.279	14.191	14.381	<0.001	6614	11.06
Arboreal (+2°C)	13.393	13.298	13.478	<0.001	6614	
Arboreal (+4°C)	11.746	11.666	11.830	<0.001	6614	
Aquatic (current)	17.408	17.352	17.471	<0.001	14091	
Aquatic (+2°C)	16.528	16.468	16.581	<0.001	14091	
Aquatic (+4°C)	15.287	15.225	15.346	<0.001	14091	

Table S2 | Statistical model estimates for overheating risk and the number of overheating events. Model estimates for each microhabitat (terrestrial, arboreal) and each climatic scenario (current, +2°C, or +4°C of global warming above pre-industrial levels) are depicted. The estimated number of overheating events in species predicted to experience at least one overheating event (i.e., overheating species) are also depicted. Model estimates for aquatic microhabitats are not displayed because no species was predicted to experience overheating events in this microhabitat. No contrast structure was used in the presented models. mean: mean model estimate; CI.lb: lower bound of the 95% confidence interval; CI.ub: upper bound of the 95% confidence interval; p: p-value; k_{sp}: number of genera; k_{sp}: number of species; k_{obs}: number of observations; Var_{genus}: variance explained by differences between genera; Var_{sp}: variance explained by differences between species; Var_{obs}: residual variance.

	Overheating risk									
	mean	**CI.lb**	**CI.ub**	**p**	**k_{genus}**	**k_{sp}**	**k_{obs}**	**Var_{genus}**	**Var_{sp}**	
Terrestrial (current)	9.98×10^{-7}	5.60×10^{-7}	1.78×10^{-6}	<0.001	464	5177	203853			
Terrestrial (+2°C)	1.93×10^{-6}	1.09×10^{-6}	3.43×10^{-6}	<0.001	464	5177	203853			
Terrestrial (+4°C)	9.09×10^{-6}	5.13×10^{-6}	1.61×10^{-5}	<0.001	464	5177	203853			
Arboreal (current)	4.77×10^{-7}	2.58×10^{-7}	8.80×10^{-7}	<0.001	174	1771	56210	0.306	69.653	
Arboreal (+2°C)	9.78×10^{-7}	5.45×10^{-7}	1.75×10^{-6}	<0.001	174	1771	56210			
Arboreal (+4°C)	3.72×10^{-6}	2.08×10^{-6}	6.67×10^{-6}	<0.001	174	1771	56210			
	Number of overheating events (all species)									
	mean	**CI.lb**	**CI.ub**	**p**	**k_{genus}**	**k_{sp}**	**k_{obs}**	**Var_{genus}**	**Var_{sp}**	
Terrestrial (current)	0.014	0.001	0.080	<0.001	464	5177	203853			
Terrestrial (+2°C)	0.025	0.002	0.127	<0.001	464	5177	203853			
Terrestrial (+4°C)	0.153	0.046	0.460	<0.001	464	5177	203853			
Arboreal (current)	0.008	0.001	0.043	<0.001	174	1771	56210	0.110	52.500	
Arboreal (+2°C)	0.015	0.001	0.083	<0.001	174	1771	56210			
Arboreal (+4°C)	0.076	0.012	0.230	<0.001	174	1771	56210			
	Number of overheating events (among overheating species)									
	mean	**CI.lb**	**CI.ub**	**p**	**k_{genus}**	**k_{sp}**	**k_{obs}**	**Var_{genus}**	**Var_{sp}**	**Var_{obs}**
Terrestrial (current)	2.155	0.239	5.264	<0.001	38	104	836			
Terrestrial (+2°C)	2.576	0.410	5.857	<0.001	61	168	1424			
Terrestrial (+4°C)	6.747	3.136	11.385	<0.001	118	391	4248			
Arboreal (current)	1.621	0.026	4.429	<0.001	4	13	152	0.253	0.187	0.310
Arboreal (+2°C)	1.956	0.113	4.973	<0.001	5	16	283			
Arboreal (+4°C)	5.084	1.806	9.387	<0.001	17	56	748			

Table S3 | Statistical model estimates for the number of species predicted to experience overheating events. Model estimates for each microhabitat (terrestrial, arboreal) and each climatic scenario (current, +2°C, or +4°C of global warming above pre-industrial levels) are depicted. The estimated number of species overheating in assemblages containing at least one species predicted to experience at least one overheating event (i.e., overheating assemblages) are also depicted. Model estimates for aquatic microhabitats are not displayed because no species was predicted to experience overheating events in this microhabitat. No contrast structure was used in the presented models. mean: mean model estimate; CI.lb: lower bound of the 95% confidence interval; CI.ub: upper bound of the 95% confidence interval; p: p-value; k_{obs}: number of observations; Var_{obs}: residual variance.

	Number of species overheating (all assemblages)					
	mean	**CI.lb**	**CI.ub**	**p**	**k_{obs}**	**Var_{obs}**
Terrestrial (current)	0.056	0.016	0.118	<0.001	14090	55.47
Terrestrial (+2°C)	0.096	0.029	0.199	<0.001	14090	
Terrestrial (+4°C)	0.288	0.083	0.604	<0.001	14090	
Arboreal (current)	0.021	0.002	0.054	<0.001	6614	
Arboreal (+2°C)	0.040	0.006	0.094	<0.001	6614	
Arboreal (+4°C)	0.107	0.021	0.243	<0.001	6614	
	Number of species overheating (among overheating assemblages)					
	mean	**CI.lb**	**CI.ub**	**p**	**k_{obs}**	**Var_{obs}**
Terrestrial (current)	3.185	0.601	6.883	<0.001	253	0.601
Terrestrial (+2°C)	3.228	0.678	6.810	<0.001	426	
Terrestrial (+4°C)	3.084	0.617	6.557	<0.001	1328	
Arboreal (current)	1.930	0.054	5.054	<0.001	74	
Arboreal (+2°C)	2.445	0.189	5.649	<0.001	111	
Arboreal (+4°C)	2.509	0.312	5.692	<0.001	285	

Table S4 | Statistical model estimates for the proportion of species predicted to experience overheating events. Model estimates for each microhabitat (terrestrial, arboreal) and each climatic scenario (current, +2°C, or +4°C of global warming above pre-industrial levels) are depicted. The estimated proportion of species overheating in assemblages containing at least one species predicted to experience at least one overheating event (i.e., overheating assemblages) are also depicted. Model estimates for aquatic microhabitats are not displayed because no species was predicted to experience overheating events in this microhabitat. No contrast structure was used in the presented models. mean: mean model estimate; CI.lb: lower bound of the 95% confidence interval; CI.ub: upper bound of the 95% confidence interval; p: p-value; k_{obs}: number of observations; Var_{obs}: residual variance.

	Proportion of species overheating (all assemblages)					
	mean	**CI.lb**	**CI.ub**	**p**	**k_{obs}**	**Var_{obs}**
Terrestrial (current)	1.22×10^{-5}	8.96×10^{-6}	1.66×10^{-5}	<0.001	14090	42.26
Terrestrial (+2°C)	2.09×10^{-5}	1.60×10^{-5}	2.72×10^{-5}	<0.001	14090	
Terrestrial (+4°C)	8.13×10^{-5}	6.60×10^{-5}	1.00×10^{-4}	<0.001	14090	
Arboreal (current)	1.19×10^{-5}	7.07×10^{-6}	2.02×10^{-5}	<0.001	6614	
Arboreal (+2°C)	1.86×10^{-5}	1.19×10^{-5}	2.89×10^{-5}	<0.001	6614	
Arboreal (+4°C)	4.99×10^{-5}	3.62×10^{-5}	6.87×10^{-5}	<0.001	6614	
	Proportion of species overheating (among overheating assemblages)					
	mean	**CI.lb**	**CI.ub**	**p**	**k_{obs}**	**Var_{obs}**
Terrestrial (current)	0.053	0.046	0.061	<0.001	253	1.019
Terrestrial (+2°C)	0.058	0.052	0.065	<0.001	426	
Terrestrial (+4°C)	0.094	0.088	0.100	<0.001	1328	
Arboreal (current)	0.038	0.029	0.050	<0.001	74	
Arboreal (+2°C)	0.054	0.043	0.067	<0.001	111	
Arboreal (+4°C)	0.061	0.053	0.070	<0.001	285	

Table S5 | Statistical model estimates for the association between the number of overheating events and thermal safety margins. Model estimates for each microhabitat (terrestrial, arboreal) and each climatic scenario (current, +2°C, or +4°C of global warming above pre-industrial levels) are depicted. Model estimates for aquatic microhabitats are not displayed because no species was predicted to experience overheating events in this microhabitat. All model estimates are on the log scale. Separate models were fitted for each microhabitat and climatic scenario. mean: mean model estimate; se: standard error; p: p-value; k_{sp}: number of genera; k_{sp}: number of species; k_{obs}: number of observations; Var_{genus}: variance explained by differences between genera; Var_{sp}: variance explained by differences between species; Var_{obs}: residual variance.

	mean	**se**	**p**	**k_{genus}**	**k_{sp}**	**k_{obs}**	**Var_{genus}**	**Var_{sp}**	**Var_{obs}**
Terrestrial (current)									
Intercept	3.723	0.390	<0.001	464	5177	203853	5.850	3.346	0.116
Slope (TSM)	-1.201	0.031	<0.001						
Terrestrial (+2°C)									
Intercept	6.318	0.310	<0.001	464	5177	203853	5.272	2.380	0.078
Slope (TSM)	-1.452	0.027	<0.001						
Terrestrial (+4°C)									
Intercept	7.611	0.171	<0.001	464	5177	203853	2.954	1.025	0.248
Slope (TSM)	-1.616	0.015	<0.001						
Arboreal (current)									
Intercept	4.929	1.091	<0.001	174	1771	56210	0.001	15.190	0.001
Slope (TSM)	-1.511	0.094	<0.001						
Arboreal (+2°C)									
Intercept	7.836	0.836	<0.001	174	1771	56210	4.359	2.358	0.001
Slope (TSM)	-1.739	0.080	<0.001						
Arboreal (+4°C)									
Intercept	10.093	0.587	<0.001	174	1771	56210	8.789	0.917	0.001
Slope (TSM)	-2.085	0.039	<0.001						